catalysts

MDPI

Review

Balancing Photocatalytic and Photothermal Elements for Enhanced Solar Evaporation—A Review

Daniela Meroni [1,2], Hady Hamza [1], Vanni Lughi [3] and Maria Vittoria Diamanti [2,4,*]

[1] Department of Chemistry, Università degli Studi di Milano, 20133 Milan, Italy; daniela.meroni@unimi.it (D.M.); hadyahmed.hamza@unimi.it (H.H.)
[2] Consorzio Interuniversitario Nazionale per la Scienza e Tecnologia dei Materiali, 50121 Florence, Italy
[3] Department of Engineering and Architecture, Università degli Studi di Trieste, 34127 Trieste, Italy; vanni.lughi@dia.units.it
[4] Department of Chemistry, Materials and Chemical Engineering "Giulio Natta", Politecnico di Milano, 20133 Milan, Italy
* Correspondence: mariavittoria.diamanti@polimi.it

Abstract

Water is a critical resource underpinning natural, societal and economic development, and its importance will grow bigger in the next decades. Interfacial solar evaporators are a promising and cost-effective technology for the generation of freshwater from saline and polluted waters. Yet, although these devices effectively reject salts and non-volatile pollutants, the presence of volatile organic compounds in the water source may lead to low water quality of the distillate. This review addresses the introduction of photocatalytic materials in solar evaporator devices to improve water quality, highlighting in particular possible synergies and incompatibilities between the materials promoting these functionalities. The interactions of the photocatalyst with photothermal materials are described, along with an overview of the materials most commonly selected for both functionalities. A positive interaction clearly emerges, with the photothermal materials not only accelerating evaporation but also generally stimulating the photocatalytic degradation of VOCs. Limits to the implementation of such a combination are described, including those due to electrolyte content and salt accumulation, reaction rate and mass transfer. Finally, recommendations regarding testing conditions and future studies are presented.

Keywords: photocatalysis; photocatalytic oxidation; advanced oxidation processes; photothermal evaporators; solar-driven interfacial evaporators; desalination; photothermic material; solar-steam generators; wastewater treatment; pollution remediation

Academic Editor: Fernando Fresno

Received: 11 December 2025
Revised: 12 January 2026
Accepted: 27 January 2026
Published: 3 February 2026

1. Introduction

Using sunlight to obtain pure water is not an innovative idea: examples of solar stills date back to ancient civilizations, whose sailors soon understood how to exploit the huge amount of seawater surrounding them to produce drinking water for long trips. Indeed, the concept is—apparently—easy to understand and to implement, as it simply mimics Earth's hydrological cycle. In recent years, interfacial solar evaporators, which localize heat at the air–water interface rather than in the entire bulk liquid, have emerged as a natural evolution of traditional solar stills aiming at minimizing thermal losses and maximizing evaporation efficiency [1]. Yet, the apparent simplicity that drives the interest in solar evaporators technology, and more specifically in interfacial solar evaporators, breaks down when you have to deal with implementing it on a large scale.

Extensive effort has been devoted to the definition of an optimal setup allowing not only for high efficiencies, meaning high quantity of water purified per unit time and unit energy absorbed, but also for high quality of the purified water and possibly for a long lifetime of the evaporator device.

Besides a careful optimization of the device design—including the porous floating element composition, hydrophilicity/hydrophobicity and geometry, and water collection system—the choice of materials and their functionalization is no less crucial. Recent research is focusing on the development of more and more efficient thermal absorbers to boost energy conversion and, consequently, evaporation rate, which is achieved by holistic material engineering, including both chemical composition—and consequent light absorption range—and micro- and macrostructures [2–9]. Several recent reviews address the current status of solar-driven interfacial evaporator technology, from the choice of device design to materials selection, to the introduction of side functionalities like photo/electrocatalysis [1,10–15].

The introduction of photocatalytic elements to improve water quality is of particular importance when the starting water source also contains organic pollutants, which may include volatile organic compounds that would evaporate together with water, thus compromising water quality [10,16,17]. Photocatalysis is a well-known advanced oxidation process able to degrade a broad range of recalcitrant water pollutants [18,19] and volatile organic compounds [20]. Moreover, the introduction of a photocatalytic functionality would also benefit the device's long-term effectiveness, as pollutants may contaminate the active materials and therefore compromise their service [21]. Lastly, antibiofouling capabilities are welcome, as the presence of biological material in water may cause premature deactivation of the device [22–24].

Yet, such elements all rely on the absorption of sunlight. It is then important to explore possible synergies [25] and incompatibilities between the materials promoting these functionalities. In addition, treating water with high salt content can hinder the photocatalytic activity of some of the most commonly employed photocatalysts [26–28]. While most of the literature on this topic highlights the beneficial aspects of the coupling of photocatalysis and photothermal evaporation, these crucial issues have seldom been recognized. The present critical review aims to bridge this gap by critically discussing the properties of the most widely adopted photothermal and photocatalytic materials and examining possible limitations of their combination, along with strategies to mitigate them.

2. Photothermal Materials: Working Principles and Examples

We focus on photothermal materials for solar-driven interfacial evaporation technologies, where it is desirable to maximize the ability of the material to convert incident solar radiation directly into localized heat at a water–air interface. These materials are incorporated into composite structures or applied as coatings to enhance the photothermal performance of solar-driven evaporation devices. In this section, we outline the main physical mechanisms that can be exploited to drive processes, such as localized radiation-to-heat conversion, and list some key examples.

The fundamental principles of photothermal conversion can be summarized by describing the key steps of the process that transforms electromagnetic energy (light) into thermal energy (heat):

- Light absorption associated with electron excitation: Materials with a broadband absorption spectrum throughout the UV-VIS-NIR range as well as high absorption coefficients are desirable for this stage [29]. However, if a photocatalytic element is to be added, its light absorption properties should be considered, as more extensively discussed in Section 6.

- Energy relaxation via thermalization: Excited electrons rapidly return to lower (ground) energy states. For photothermal applications, materials where such relaxation occurs through non-radiative decay pathways are required [30]. Here, the relaxation energy is transferred to lattice vibrations (phonons), leading to a temperature increase in the material (thermalization).
- Heat localization and transfer: For solar-driven evaporation applications, the heat generated via light absorption and subsequent thermalization must be precisely localized at the water–air interface to maximize evaporation efficiency. Ideal photothermal materials should have an appropriate morphology to achieve this localization, such as a porous or cellular architectures at the micro- and nanoscale, designed to facilitate water transport to the evaporation surface while simultaneously providing thermal insulation to the underlying water body. The objective is to maximize evaporation rates while minimizing the energy lost by heating the bulk water [31,32].

Photothermal materials can be classified based on their chemical composition and the dominant radiation–heat conversion mechanisms.

Metal nanomaterials leverage Localized Surface Plasmon Resonance (LSPR) as the primary working principle for the radiation–heat conversion [33]. LSPR occurs when incident light interacts with free electrons within metal nanoparticles. If the frequency of the incident light matches the natural oscillation frequency of these surface electrons, a strong collective oscillation, or plasmon, is induced. This resonance leads to highly enhanced light absorption. The excited plasmons rapidly transfer their energy to lattice vibration (electron–phonon scattering), resulting in a localized temperature increase within and around the nanoparticle. The LSPR phenomenon is highly dependent on the nanoparticle size, shape, composition, and dielectric environment, allowing for tunable absorption across various parts of the solar spectrum [34].

A variety of metal nanoparticles has been investigated for photothermal applications [34]. Gold nanoparticles show excellent stability, biocompatibility, and LSPR tunability in the visible to near-infrared range and are often used not only as photothermal materials but also to enhance photocatalysts efficiency, thus addressing well interfacial solar evaporator technology [33,35–37]. In this case, plasmon-generated electrons can be injected into the conduction band of the photocatalyst, extending photoresponse into the visible light range and promoting charge separation (see Section 3) [38]. Silver nanoparticles offer strong LSPR effects and high extinction coefficients; moreover, silver is one of the most diffusely studied antibacterial materials, which is also attractive for interfacial solar evaporators [39–42]. Copper nanoparticles have a strong LSPR, providing a cost-effective alternative to other noble metals, but need stabilization against oxidation for durable utilization [43–45].

Semiconductor materials leverage mainly two distinct working principles [46]. Defect-induced localized plasmon resonance is similar to what is observed in metallic systems such as those described above and can occur in doped semiconductor materials where a high concentration of free charge carriers is available [47]. Band gap absorption followed by thermal relaxation is a more common mechanism for photothermal conversion in semiconductors and involves the direct absorption of photons with energy larger than the material's electronic band gap. This absorption promotes an electron from the valence band to the conduction band, creating an electron–hole pair. For photothermal applications, the electron–hole pairs should predominantly undergo rapid non-radiative relaxation. In this case, the excited electron loses its excess energy by exchanging it with lattice vibrations as it cascades to the bottom of the conduction band, and the hole relaxes to the top of the valence band. If the subsequent recombination of the electron and hole is of non-radiative nature thanks to defect-related processes, the remaining energy is also released as heat and is highly desirable for photothermal applications [48,49].

Copper chalcogenide semiconductors such as CuS and Cu_2S are notable for their strong absorption in the near-infrared region and efficient photothermal conversion, often exhibiting plasmon-like features [47]. Transition metals and their nitrides, carbides, borides, and sulphides (notably TiN, TiC, and various metal oxides) often possess suitable band gaps for solar absorption and robust non-radiative decay pathways, as well as chemical and thermal stability, making them effective photothermal converters for long-term applications in particular [48,49]. While photocatalytic materials also belong to semiconductors, their compositions generally do not coincide; first on account of the different radiation energies—in the UV or near-UV range—where they absorb to form reactive electron/hole pairs, and second as electron–hole pairs are required not to recombine in this case. Few exceptions to this situation, i.e., materials that can work both as photocatalysts and as photothermal absorbers, are graphitic carbon nitride (g-C_3N_4) and metal–organic frameworks (see Section 5). Indeed, g-C_3N_4 band gap edges are positioned conveniently to allow photogenerated holes and electrons to drive redox reactions necessary in the degradation of organic pollutants; at the same time, its non-radiative recombination paths also allow photothermal heat generation [50,51].

Carbon-based materials are highly attractive for photothermal applications due to their abundance, cost-effectiveness and exceptional chemical stability in challenging environments, including those with high salt, acid, or alkali concentrations [29]. The primary photothermal mechanism in carbon-based materials is associated with the delocalized π-electrons characteristic of sp^2 hybridized carbon (as found in graphitic carbon, graphene and carbon nanotubes), which enable highly efficient, broadband absorption across the entire solar spectrum, making them excellent light harvesters [29]. The fundamental energy transfer mechanism is similar to the ones described above, as the photo-excited electrons transfer their energy to lattice vibrations, a mechanism that is particularly efficient in carbon-based materials [30]. The inherent thermal conductivity of most carbon allotropes can facilitate heat spreading within the photothermal layer, while their typically porous structures can be engineered to provide effective thermal insulation to the underlying water body, promoting localized heating.

Carbon black is a simple, widely available, low-cost and highly absorbing material and is considered the benchmark for photothermal absorbers [29] for solar-based evaporation systems. Carbon nanotubes (CNTs) as well as graphene and graphene oxide (GO) have also been integrated into flexible and robust photothermal films [29], conferring outstanding mechanical properties suitable for long-term applications. Interestingly, CNTs and other carbon-based species can complement and enhance the action of photocatalysts by acting as a sink towards photogenerated electrons, which suppresses electron–hole recombination. Moreover, as seen for plasmonic nanoparticles, CNTs, graphene and GO can transfer themselves photoelectrons in the photocatalyst conduction band, extending photocatalytic activity into the visible light range [52,53].

Polymer-based materials have been recently investigated as photothermal converters due to their ease of synthesis, affordability, high light absorption capabilities, and often good biocompatibility [54]. The photothermal mechanism in polymer-based materials typically involves the absorption of incident photons by specific chromophoric units or conjugated segments within their molecular structure and concurrent generation of excited electrons. In efficient photothermal converters, electron energy is subsequently relaxed primarily by exciting vibrational modes of the polymer chains. Polymeric photoabsorbers are appreciated for their molecular design flexibility, which allows for tailoring the optical properties for optimizing light absorption in the solar spectrum and for the ease of processing.

Polypyrrole is a conducting polymer that has been investigated as photothermal material, exhibiting strong broad-spectrum absorption, particularly in the near-infrared region, and efficient photothermal conversion [54]. Polydopamine (PDA) adds biocompatibility as an interesting property for photothermal applications.

Recently, quantum dots have been only marginally investigated as potential photothermal materials, most notably in the case of carbon quantum dots for therapeutic applications, exhibiting strong light absorption in the near-infrared spectrum [55]. Little attention has been paid to the use of these kinds of nanostructures as photothermal absorbers for solar-driven evaporation applications, although some recent applications for solar desalination can be found [56]. Nevertheless, quantum dots would be expected to be excellent candidates for these applications due to the high absorption rates and the tunability of the absorption range in the UV-VIS-NIR and the potential for engineering the electronic structure [57]. In particular, core–shell nanoparticles of the so-called Inverted Type-1 kind (Figure 1) have a very strong potential for such applications. In their most fundamental form, these nanoheterostructures consist of a small core semiconductor nanoparticle, typically quasi-spherical and with a diameter in the range of 2–5 nm, coated with a thin (typically 1–3 nm) semiconductor shell. The semiconductor compositions are selected in such a way that the bulk bandgap of the shell is smaller than that of the core, and the top of the valence band of the shell material is at a higher energy than that of the core material, and vice versa for the bottom of the conduction band (this corresponds to the condition that the electron affinity of the bulk shell material is larger than that of the core). The energy structure of the system, acting as a confinement potential for electrons and holes, is the one depicted in the bottom panel of Figure 1. By tuning the composition and size of the core and the shell, it is possible to engineer the probability of finding electrons and holes (blue continuous lines in the Figure 1) to be highest in the shell. In such a system, the highest occupied electron energy level of the nanoheterostructure (A in the Figure 1) falls at intermediate energy values between the top of the valence bands of the core and the shell, while the lowest unoccupied level (B) falls between the bottom of the conduction bands.

On the one hand, therefore, the photon absorption of the system, associated with the energy separation between these electron energy levels, can be tuned to best match the solar spectrum by appropriately selecting the size and composition of the core and the shell, thus maximizing the number of photogenerated electrons and holes.

On the other hand, the ability of herding these electrons and holes in the shell, i.e., in close proximity to the outermost surface of the nanoparticle where a large concentration of defects is found, maximizes the probability of non-radiative recombination paths, thus favoring the localized generation of heat.

Interestingly, similar nanostructures with different energy structures (such as Type 1, Type 2 and quasi-Type 1) have a high potential for the enhancement of photocatalytic activity, making quantum dots highly versatile systems for solar-driven evaporation devices from several different standpoints.

Yet, at this time, only carbon black and metallic nanoparticles show the potential for immediate scalability at the industrial level for application in solar-driven evaporation devices. Semiconductor materials, especially in the form of nanoparticles, and polymer-based materials–while in many cases are quite advanced at the laboratory or pilot scale–are expected to need further development from the processing and product integration point of view.

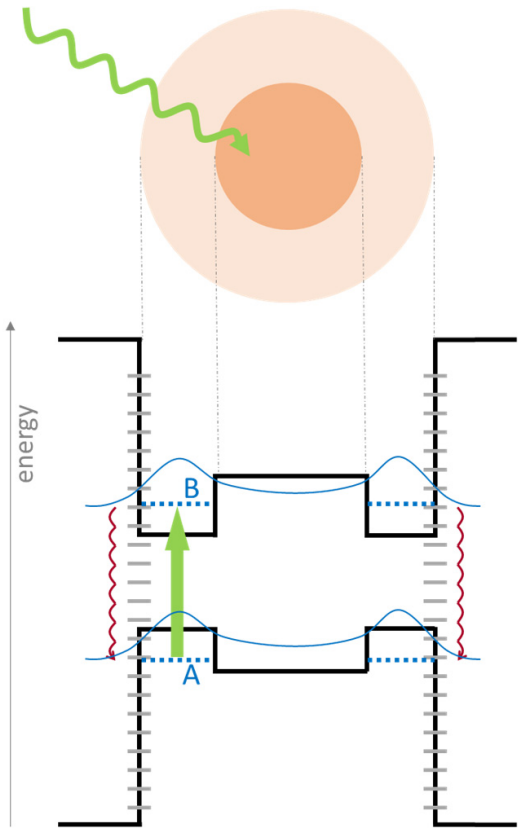

Figure 1. (**Top**) Schematics of an Inverted Type-1 quantum dot interacting with a visible photon, constituted by a nanometric semiconductor core and covered by a thin semiconductor shell with a lower energy bandgap. (**Bottom**) Energy structure of the quantum dot. The photon excites an electron from the highest occupied energy level A to the lowest unoccupied level B (green arrow), leaving a hole in A. The peculiar energy potential shape (depicted in black) created by the Inverted Type-1 structure enhances the probability (blue curves) for the electrons and holes to be found near the external, highly defective surface of the quantum dot. The large quantity of defect-associated energy levels (gray short segments) promotes non-radiative recombination paths (red arrows) associated with heat generation.

3. Photocatalytic Materials: Working Principles and Examples

After more than 100 years since the first appearance of the word "photocatalysis" in the scientific literature [58–62], with early works observing the fading of dyes and pigments in contact with some oxides [63], and 53 years after the cornerstone publication from Fujishima and Honda [64], photocatalysis is now a mature technology from a scientific standpoint, with more than 25 k articles published in 2024 (keyword: "photocatal *", source: Scopus, as of October 2025) and an ever-growing trend (Figure 2a).

Photocatalysis has been defined in a huge number of reviews: just to give a reference, more than 2000 reviews were published on the topic of photocatalysis only in 2025, and a big part of them contained a summary of how the process works. While a clear insight of energy transfer mechanisms inside the semiconductor are still under debate [65], the overall photoactivation mechanism can be simply described as follows. Briefly, a semiconductor is activated by the absorption of light of proper energy—specifically, equal or higher to the photocatalyst bandgap. This allows an electron of the valence band to move to the material conduction band, thus creating an electron–hole couple. This in turn may undergo two main paths: either the two photogenerated carriers react with other species present at the photocatalyst surface, generally water and oxygen molecules, or they recombine, releasing heat. In the former case, reactive radicals are formed, which can promote several

chemical reactions, including the oxidation of organic molecules (Figure 3) [66–70]. This mechanism is very efficiently set up by many semiconductor materials, among which titanium dioxide, TiO_2, is by far the most studied from both a scientific and an industrial perspective, with most commercial products based on this material [71,72].

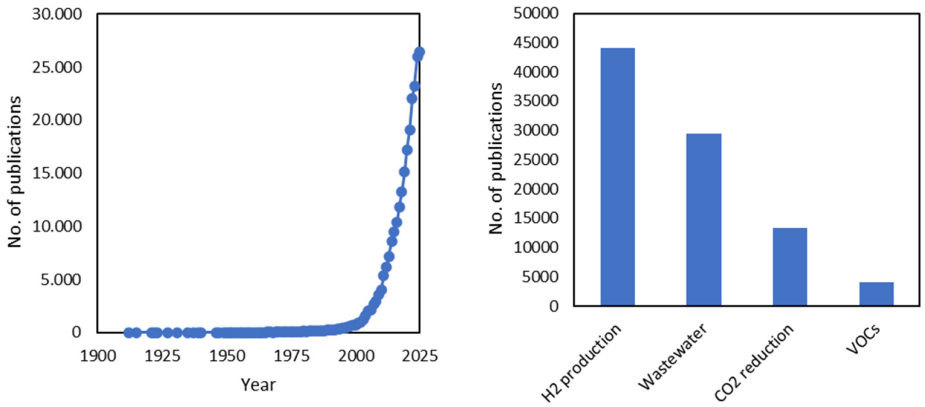

(**a**) (**b**)

Figure 2. Literature analysis: (**a**) number of articles published on "photocatal *" during the years; (**b**) number of articles published in the last 10 years, by specific photocatalysis topical area.

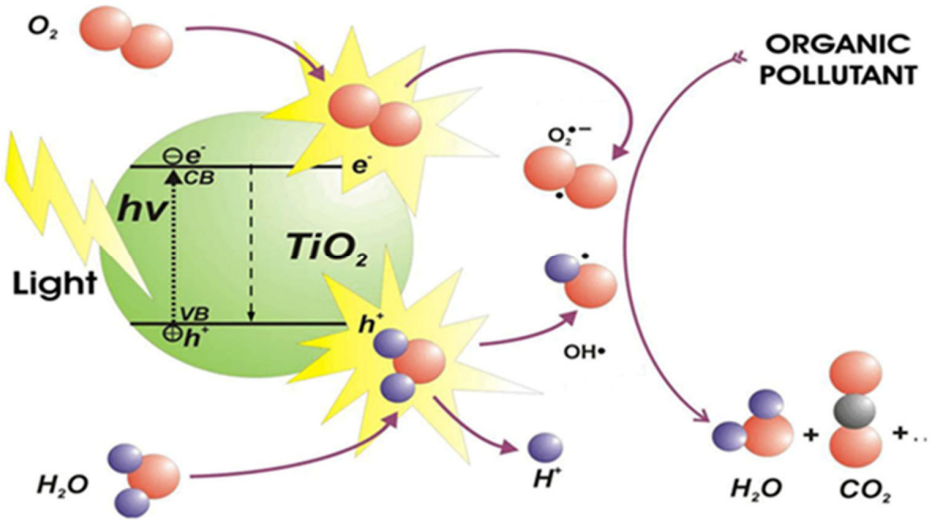

Figure 3. Schematic diagram of the principles of photocatalysis. Reprinted with permission from [61].

Indeed, for decades TiO_2 has been the main subject of research in the field of photocatalysis, in the form of nanoparticles [73–75], films [76–78], or membranes [79–82], produced via chemical synthesis routes [77,83–85], physical deposition [78,86,87], or electrochemically [26,88–90]. Given its relatively high bandgap, which only allows light absorption in the near-UV range, much effort has been devoted to the extension of light exploitation through strategies such as doping, reduction or heterojunction formation [74,91–96]. In parallel, other photocatalysts have been widely addressed that account for a smaller bandgap, thus allowing light absorption in the visible range: these materials include other oxides such as ZnO, $BiVO_4$, Bi_2O_3, MnO_2 and CuO [97–102], metal–organic frameworks [103,104], graphitic carbon nitride (g-C_3N_4) [105] and several hybrid nanocomposites between two semiconductors [93], a semiconductor and noble metals to exploit plasmon resonance effects [96], or a semiconductor and carbon-based species, such as rGO, GO, CNTs and carbon quantum dots [106]. Many of these materials were already addressed in the previous section (see Section 2), as they provide combinations of photocatalytic and photothermal

effects either within the same material or through the combination of two different ones. Although such photocatalysts exhibit better light exploitation performances, their industrial application is limited by the more complex production, availability, or stability.

At an industrial level, photoactive materials are on the market of building materials such as cements (Heidelberg *TioCem*®, Italcementi *TiX Activ*™), glass (Pilkington *Activ*™, Saint-Gobain *Bioclean*®) and ceramics (TOTO *Hydrotect*™, Iris Ceramica *Active Surfaces*®). Other commercially available solutions based on photocatalysis are air purification materials (paints and coatings proposed by a variety of producers) and devices for industrial applications—like the ones produced by BMB Technologies and Services and Airpurtec-and for household use—with plenty of big and small players in the field of air conditioning and purification. The application of photocatalysis to water purification still has not fully found a clear industrial collocation, although many pilot projects have been successfully produced.

Indeed, the applicability of photocatalysis to real-life operations is less immediate due to the complexity of actual water matrices and environmental conditions, as well as to the intrinsic nature of photon-driven processes, where large reactors suffer from low light penetration [107,108]. In fact, although advanced oxidation processes (AOPs) are employed in the last step of the purification treatment, after primary treatments to remove suspended solids and fats/oils and secondary ones to reduce organic matter, nitrogen and phosphorus [109,110], highly polluted waters can still lead to photon attenuation. This effect can be countered by using suitable flow reactor geometries, such as capillary microreactors, and numbering up reactor chambers [111]. Still, most demonstrations of the effectiveness of such a strategy refer to photochemical synthesis or oxidation reactions rather than to water purification [107,112,113]. Studies dedicated to pilot-scale photocatalytic water treatment are increasing but either consider the coupling of photocatalysis with other AOPs, like photo-Fenton or biological ones [114,115], or lead to results consistently lower than those achieved in laboratory ones [116–120].

Probably accounting on this difficulty, i.e., since much work is still needed to upscale the liquid phase applications, a recent literature analysis indicates an exactly opposite profile, with water purification works largely outnumbering gas phase targets (Figure 2b). Considerable attention is also dedicated to hydrogen production and CO_2 reduction, which are not considered in this review.

Interestingly, among the thousands of works published yearly on photocatalysis, only 1% is dedicated to the use of this technology inside solar evaporators, indicating this application is still at its early stage of understanding.

The next paragraphs address more directly pros and cons of multifunctional solar evaporators.

4. Benefits of Coupling Photothermal and Photocatalytic Materials

As a matter of fact, photocatalysis implies the acceleration of a chemical reaction through the production of reactive species on the surface of a photocatalyst. It has been proposed that the heat accumulation arising from the combined presence of a photothermal material can promote the photocatalytic pathways via different mechanisms. Localized heat can boost mass transfer, improving the supply of the limiting reactant(s), as well as decrease desorption energy barriers, suppressing the accumulation of byproducts and catalyst poisons [25]. It has also been proposed that heat could stimulate positive non-linearities in photo-conversion efficiency over plasmonic catalysts [121]. Moreover, the combination of photocatalysis and thermal catalysis has been suggested to be able to promote certain reactions by lowering their apparent activation energy [122,123]. Not only is the individuation of specific mechanisms is still under debate, but the nomenclature

itself is sometimes confusing, as reported in recent reviews [25,124]: here, we focus on situations involving a photoactive semiconductor, capable of promoting photodegradation reactions itself, in the presence of an added thermal input, excluding pure thermal catalytic systems [25]. Since this cooperation is effective in decreasing the apparent activation energy, or in accelerating the supply of limiting reactants, an increase in overall reaction rate/quantum efficiency is highlighted, for instance, in [125–128]. Interestingly, Ye et al. observed a decrease in TiO_2 photoreforming activity with increasing temperature from 20 to 40 °C and, conversely, an improvement with Pt loading, which also increased the temperature in the same range [129]. To be noted here, and in similar works [130], the difficulty is in disentangling different photoactivated mechanisms: in fact, Pt is not only acting as photothermal absorber but also improving TiO_2 charge carriers separation, thus making it impossible to disentangle the two inputs and quantify the photothermally induced benefit.

In suitable materials, a temperature gradient can also generate a pyroelectric effect, with the formation of a pyro-potential across the material which enhances charge separation, further pushing reaction kinetics [131–133]. The combination of photocatalysis and photothermal heating has also been shown to promote bacterial inactivation, which can be highly beneficial for preventing biofouling in solar interfacial evaporators [134]. Conversely, the possible effect of bandgap narrowing driven by the temperature increase only affects the process marginally [135].

All these elements could concur to increase degradation reaction kinetics, although parallel negative effects may lead to a different fate, such as a promoted desorption of the pollutant or of its intermediates or even photocatalyst thermal degradation in case of thermally sensitive (non-oxide) materials [136].

5. Trends in Literature Studies on Photocatalytic-Photothermal Evaporators

5.1. Materials

Table 1 reports a summary of the materials whose use is most frequently reported in solar evaporators, either as photothermal elements, or as photocatalysts, or both. As emerges from its observation, it is clear that the use of carbon species as a photothermal element is widely appreciated, while the most diffuse photocatalyst is by far TiO_2, followed by bismuth-based species. This analysis of the recent literature shows that in almost all cases, the combination of the two materials enhances photodegradation rather than suppressing it (Table 1), and no improvement is observed in only in a limited number of cases. Furthermore, although most evaporating systems rely on different components to achieve the two effects, it is indeed possible to concentrate both functionalities in one same material. It is the case of graphitic carbon nitride, g-C_3N_4 [137–140], as well as metal–organic frameworks (MOFs) [41,103,141] and less studied compounds such as carbonized chitosan [142,143].

Table 1. Literature analysis of integrated photothermal (PT)-photocatalyst (PC) materials in interfacial solar evaporators.

PT Class	Active Material(s) Proposed	PT Material	PC Material	PT + PC Enhancement	Evaporation Rate ($kg \cdot m^{-2} \cdot h^{-1}$)	Target PC Molecule	Ref.
Noble metal based	Silk fibroin/Ag_2S/Ag_3PO_4	Ag_2S	Ag_3PO4	-	2.86 @1 sun	Phenol	[144]
	Ag-MOF	Ag-MOF	Ag-MOF	-	1.92 @1 sun	RhB	[41]
	AuNP@TiO_2	AuNP	TiO_2	Yes	1.3 mg/s @5 sun	RhB	[35]
	AAO@AuNP@TiO_2	AuNP	TiO_2	No	5 @6.7 sun	RhB	[145]
	AuNP@ZnO	AuNP	ZnO	-	1 @1 sun	RhB	[146]
	TiO_2/CuO/Cu	CuO	TiO_2	Yes	1.28 @1 sun	Phenol	[147]
	Chitosan/PAA/CuS	CuS	Chitosan	-	2.79 @1 sun	MB	[148]
	CuS@CNF/PVA	CNF	CuS	-	3.2 @1 sun	Dyes	[149]
	PPy/CuO	CuO	PPy	-	1.48 @1 sun	MB	[150]

Table 1. *Cont.*

PT Class	Active Material(s) Proposed	PT Material	PC Material	PT + PC Enhancement	Evaporation Rate ($kg \cdot m^{-2} \cdot h^{-1}$)	Target PC Molecule	Ref.
Carbon based	TiO_2 on carbon	C	TiO_2	Yes	1 @1 sun	Phenol	[151]
	$Cu/W_{18}O_{49}$@Graphene	Graphene	$W_{18}O_{49}$	Yes	1.41 @1 sun	Phenol	[152]
	Fe_3O_4/CNT	CNT	Fe_3O_4	Yes	1.76 @1 sun	Tetracycline	[153]
	NiO-TiO_2-CNT	CNT	NiO-TiO_2	-	2.25 @1 sun	Phenol	[154]
	Mn@g-C_3N_4/PANI/carbon	g-C_3N_4/PANI/C	Mn@g-C_3N_4	No	2.99 @1 sun	Phenol	[155]
	rGO + g-C_3N_4	rGO + g-C_3N_4	g-C_3N_4	-	2.55 @1 sun	Dyes	[156]
	TiO_2@C/PAM	C	TiO_2	No	2.97 @1 sun	MB	[157]
	Carbonized sodium alginate/TiO_2	C	TiO_2	-	2.11 @2.5 sun	RhB	[158]
	TiO_2/SWCNTs/ Polyacrylamide	CNTs	TiO_2	-	3.53 @1 sun	MB	[159]
	N-TiO_2/C	C	TiO_2	-	1.73 @1 sun	RhB	[160]
	N-Fe_2O_3/carbon	C	N-Fe_2O_3	Yes	1.53 @1 sun	MB	[161]
	PVDF/TiO_2/GO	PVDF/GO	TiO_2	-	1.48 @1 sun	RhB	[162]
	GO/TiO_2/PANI	GO/PANI	TiO_2	Yes	2.81 @1 sun	Dyes, antibiotics	[163]
	MoO_{3-x} + BiOCl + CNTs	MoO_{3-x}, CNTs	BiOCl	-	7.75 @5 sun	Toluene	[164]
	BiOBrI on carbon	C	BiOBrI	-	1.67 @1 sun	Phenol	[165]
	Graphene/PPY	Graphene, PPY	PPY	Yes	2.08 @1 sun	Phenol	[166]
Other	TiO_2−PDA/PPy/cotton	PPY	TiO_2	Yes	1.55 @1 sun	MO	[167]
	Ag-PPy-TiO_2	PPy	TiO_2	Yes	1.8 @1 sun	MO	[168]
	BiOI/Bi_2S_3/PVA	Bi_2S_3	BiOI	-	2.34 @1 sun	Cr (VI)	[169]
	TiO_{2-x}/BiOI	BiOI	TiO_{2-x}/BiOI	No	2.5 @1 sun	RhB	[170]
	PPy/BiVO4-PI/MXene	PI/MXene	PPY/BiVO4	-	1.64 @1 sun	Dyes	[171]
	Ti_3O_5/PVA/PAM	Ti_3O_5	Ti_3O_5	-	4.34 @1 sun	MB	[172]
	Carbon-doped g-C_3N_4	g-C_3N_4	g-C_3N_4	-	1.64 @1 sun	Tetracycline	[173]
	SnSe@SnO_2	SnSe	SnO_2	Yes	1.19 @1 sun	RhB	[174]
	TiO_2/Ti_3C_2/C_3N_4/PVA	Ti_3C_2/C_3N_4	TiO_2	Yes	1.54 @1 sun	Phenol	[175]
	Ti_3C_2 MXene + CdS	Ti_3C_2	CdS	Yes	1.8 @1 sun	RhB, phenol	[176]
	TiO_2 on SiO_2	SiO_2	TiO_2	-	1.71 @1 sun	Phenol	[16]
	$MnFeO_3$	$MnFeO_3$	$MnFeO_3$	-	2.28 @1 sun	Dyes	[177]
	MXene-TiO_2-Ag	MXene	TiO_2	Yes	3.09 @1 sun	Phenol	[42]
	$LaCoO_3$/MoS_2	MoS_2	$LaCoO_3$	Yes	5.27 @1 sun	Dyes, phenol	[178]
	MnO_2-TiO_2	MnO_2	TiO_2	Yes	1.68 @1 sun	MB	[179]
	Bi_2MoO_6/polydopamine	Polydopamine	Bi_2MoO_6	-	2.1 @1 sun	RhB	[180]

Photocatalysis tests reported in the literature works reported in Table 1 are performed against various molecules, not necessarily volatile—although all works focus specifically on solar evaporator applications. Target pollutants are either dyes or phenol, or sometimes other more complex substances, like tetracycline or other antibiotics. When phenol is addressed, its degradation is evaluated in terms of rejection in the distillate, i.e., by measuring the final concentration in the evaporated water; instead, dye degradation is evaluated in the starting water source—as dyes are not volatile, they would not reach the distillate anyway. Indeed, it holds an interest to address both volatile and non-volatile pollutants: while volatile ones risk to evaporate together with water, thus affecting the quality of water produced, the degradation of non-volatile compounds can still be useful to improve the quality of the residual water, as well as to reduce pollution of the evaporator active element and thus extend its service life, decreasing the risks of deactivation. Based on these considerations, we have recently proposed a dual-testing strategy to comprehensively assess the device's performance: (i) studying the photocatalytic performance using dyes and monitoring their concentration in the feedwater; (ii) evaluating VOC rejection by tracking the concentration of phenol and its reaction intermediates in the distillate [181].

Still, it is very difficult to compare the photodegradation efficiency of materials listed in Table 1, on account of the different experimental conditions employed in the works. While most of the works where phenol degradation is addressed show at least some common points, from phenol concentration (10 mg/L in most cases) to light intensity (1 sun), dye degradation experiments are less similar. Moreover, some works evaluate the photocatalytic efficiency of the material in powder form, while others examine the full floating device. Eventually, most of the degradation efficiency values are provided in terms of percent degradation, which is dependent on irradiation time, intensity and

geometry, instead of providing information on reaction kinetic constants or quantum yields. Another critical point limiting comparability is the actual amount of photocatalyst in the tested device and the dark adsorption performance, which are often not reported. For these reasons, efficiencies are not reported in Table 1, as they would not be comparable.

Nevertheless, from the analysis of photocatalytic experiments collected in these works it is possible to state that whenever the study assessed the photocatalyst first, and then its combination with the photothermal element, the result was an increase in photodegradation efficiency, to a larger or smaller extent depending on the initial activity of the photocatalyst (Figure 4), with very few exceptions where the photothermal element proved neutral.

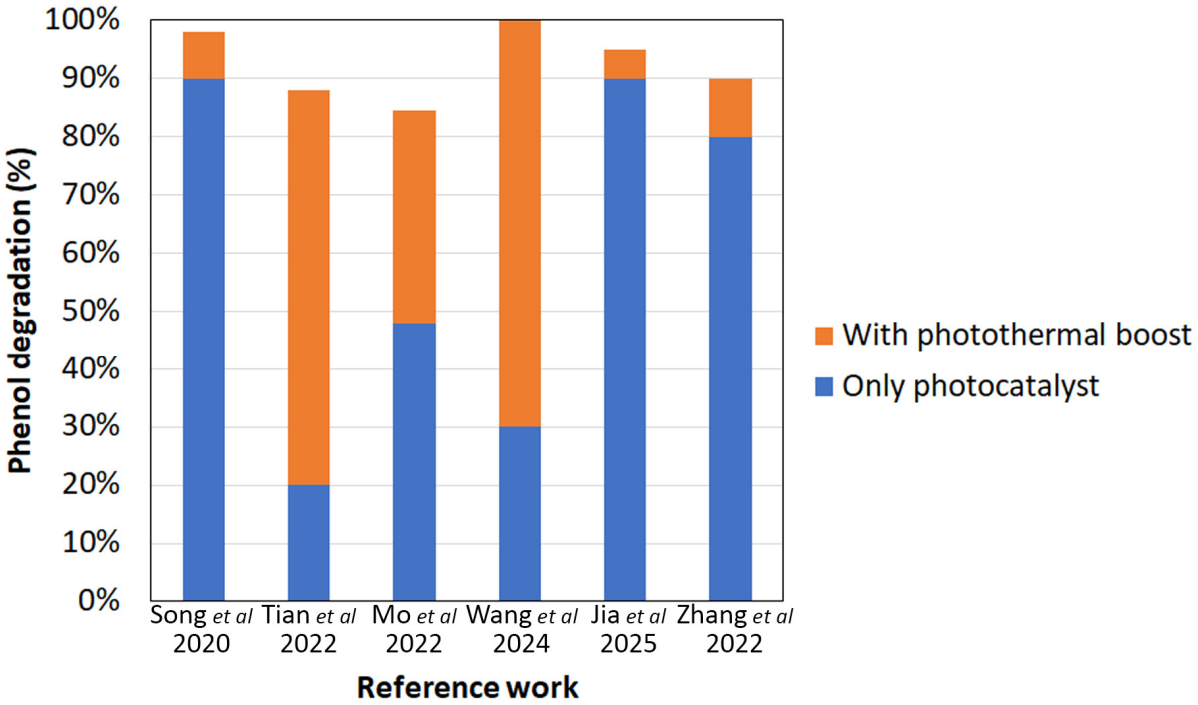

Figure 4. Increase in photocatalytic degradation efficiency as a consequence of the coupling with a photothermal element. For homogeneity, only works providing information on phenol degradation were considered. Data refer to phenol final concentration in the distillate and are extracted from [16,147,175,176,178,182].

One further note concerns the relationship between evaporation and purification efficiencies: not all systems are able to reach an optimal performance in both aspects, which means that either the evaporation will be fast but with limited purity of the resulting water, or water quality will be excellent but its production slow. This may happen when the composite photothermal/photocatalytic material needs different composition or production parameters—e.g., different ratio of active materials—to optimize evaporation vs. pollutant removal, therefore leading to the need for a compromise between the two features to achieve good effectiveness in both [144].

5.2. Testing Conditions

As for evaporation efficiency, most of the articles use homogeneous conditions at least for irradiation intensity, always providing a value of evaporation rate at 1 sun. However, in pollutant rejection and photocatalytic tests, evaporation geometries and methods are once again very variable, since they are related with solar still geometry for water collection. Moreover, actual testing conditions are often not fully described, hindering a direct comparison of evaporation efficiency [181]. Even in the presence of equal irradiation

intensity, efficiency strongly depends on geometry; therefore, the same material used in a hemispherical configuration or in a single solar still, or again in a simple beaker, would produce large differences in evaporation rate (Figure 5).

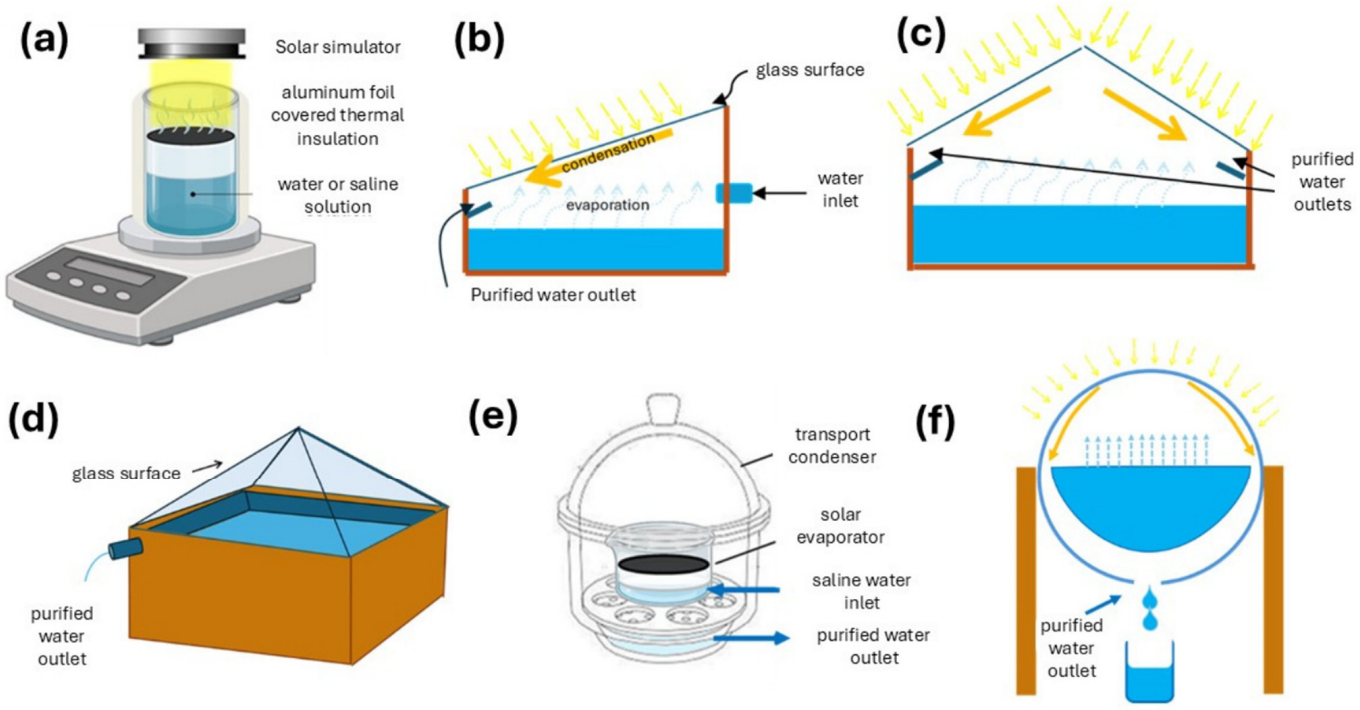

Figure 5. (**a**) Setup for photothermal efficiency determination under solar simulator; (**b**–**f**) different designs of solar stills for tests of rejection of salts and volatile organic compounds: (**b**) single-surface solar still, (**c**) double-surface solar still, (**d**) square pyramidal surface solar still, (**e**) dome-shaped still, and (**f**) spherical solar still. Reprinted with permission from [181].

The insulation and water supply efficiency provided by the support material also influence the performance: in the materials column of Table 1, reference is made only to the photothermal component, but the whole floating element is responsible for the evaporation process. While the geometry exerts such an important effect, the presence of salts or pollutants only moderately affects water evaporation rate—although always in a negative way, on account of the increase in evaporation enthalpy caused by the presence of a non-volatile solute (Figure 6) [183]—and it is generally addressed separately, after first characterizing the evaporation of pure water [41,42,147,166,177,178]. Interestingly, there is no dependence of evaporation efficiency decay on the initial performance (Figure 6). Variations may be larger at higher salt content, or for longer testing time [42,177,178]. Salt rejection is such an important theme that several reviews have been specifically dedicated to it, and reference can be made to such works for further details and metrics [184–186].

Another important point that is often neglected is the instability of efficiency over time: a high evaporation rate measured in the initial minutes of exposure with short duration tests may not coincide with the device's actual behavior in steady conditions but rather represent the maximum efficiency of materials utilized in their pristine state. The efficiency reduction in time may be a consequence of many factors, mainly the accumulation of salts, the loss of temperature gradients with prolonged use and the absorption in the hydrophilic element of pollutants that slow down water supply at the evaporation interface.

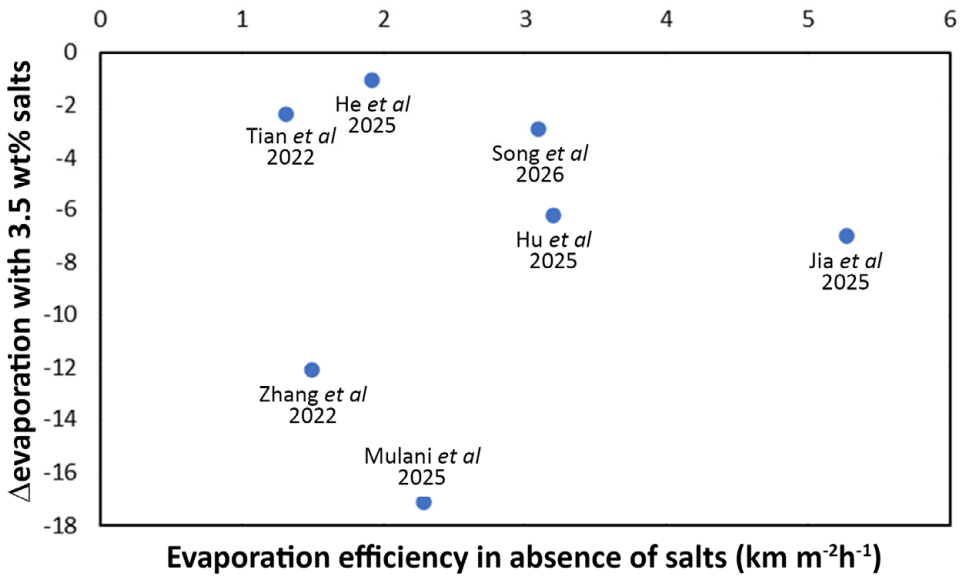

Figure 6. Evaporation efficiency decrease caused by presence of 3.5% salts, as observed in different works, as a function of the efficiency measured in absence of salts. Data extracted from [42,43,147,149,177,178,182].

5.3. LCA

On account of all the aspects abovementioned, and with special reference to the impact of the materials selected, the methods used to produce them and their possible performance decay over time, a major role in understanding the actual feasibility of using interfacial solar evaporators for water purification on a large scale can be provided by life cycle assessment (LCA) studies. Indeed, sometimes materials used in studies with desired positive relapses on the environment are themselves posing a threat to the environment, either because they are intrinsically hazardous (for their structure, e.g., high aspect ratio nanomaterials, or for their composition, e.g., Hg- or Cd-containing compounds) or are so on account of an energivorous production route. Very few works have started accompanying evaporation measurements with an analysis of the environmental impact of the materials used; generally, a benefit emerges from the use of waste or biomass-derived photothermal materials [187–189], while introducing critical raw materials such as lithium can have a large impact on the calculated impact [190]. Other works apply LCA to different solar evaporation systems, such as membrane evaporators, but considerations drawn in such works are difficult to transfer to interfacial solar evaporators, as they do not focus on the device performance but rather compare them with conventional evaporation systems requiring an electrical supply [191–194]. In this perspective, an interesting work by Jijakli et al. compares the environmental impact of water delivery to rural communities by three methods: brackish groundwater purification through solar stills, PV-powered reverse osmosis (RO) of the same groundwater and water delivery by truck from a RO plant [195]. PV-powered RO appears to guarantee the lowest environmental impact; still, it should be noted that a simple steel solar still is considered here, while interfacial solar evaporators offer better performances [196], thus decreasing the gap and potentially outperforming the RO-based technology.

Still, many factors are not yet accounted for: in fact, LCA can include different steps, and most of the current works limit the analysis to the functional application, disregarding both the performance decay that the materials necessarily experience in time and end of life, which is particularly onerous when nanomaterials are involved.

6. Limitations of Combined Photocatalytic-Photothermal Evaporators

Although integrating photoactive materials with different functionality seems promising, as explained in the previous section, some limits remain, which do not arise from single material combination but rather from device implementation.

One first point relates to salt rejection. Not all water sources to be decontaminated come from seawater, but many of them do, and in this case the intention of a solar evaporator is not only, and not mainly, that of removing pollutants but most importantly that of rejecting the excess salt that hinders the use of that water source [21,184,185,197]. In such a case, the introduction of a photocatalyst may not lead to positive results: in fact, salts tend to deactivate the photocatalyst and reduce its efficiency, making it imperative to modify the design to avoid salt–photocatalyst interferences [28,198,199]. However, most photocatalytic tests in solar evaporators are carried out in water with low electrolyte content, and the issue of electrolyte interference with photocatalysis is seldom considered [182,200,201].

One possible solution is that of reducing the direct contact between the water source and the photocatalyst, focusing the contact at the evaporation interface, with the interposition of a hydrorepellent floating element [202]—as seen in Janus-type water evaporators (Figure 7): this partially reduces the contact of the active element with salts [182,200,201]. Further help in this configuration can also come from the introduction of suitable channels or slopes that convey salts released by evaporating water in specific areas, avoiding their accumulation on the active surface [184,203,204]. Strategies based on salt redissolution might favor lower salt concentrations close to the photocatalyst surface and promote mass transfer.

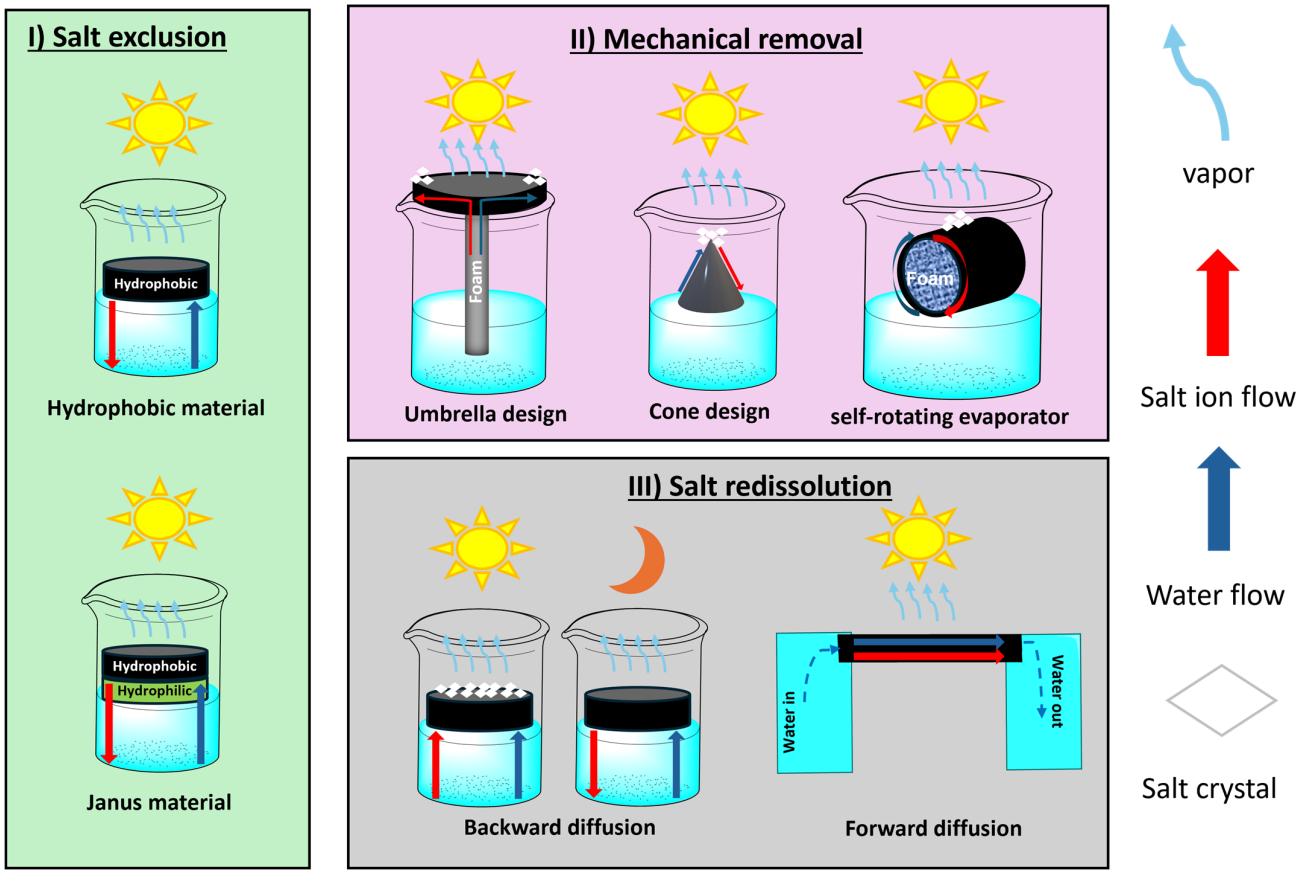

Figure 7. Salt rejection systems as proposed in the literature. Typical systems are based on the three principles reported here: (**I**) salt exclusion, (**II**) mechanical removal (by gravity or centrifugal forces), (**III**) salt redissolution (relying on diffusion driven by concentration gradients).

The possible disadvantage observed at the evaporating interface is stronger if we consider a photocatalyst designed to be immersed in the feedwater, a choice sometimes operated to also obtain the purification of the starting water basin. The unavoidable decrease in photocatalyst efficiency in the presence of salts strongly limits the degradation of pollutants in the starting water, thus hampering the beneficial effects mentioned in the previous section [41,42,149,178].

It is then clear that a photocatalyst immersed in water may often pose a limit to the purification potential of the device. On the other hand, positioning the photocatalyst on top of the floating element is not a choice without concerns: if, on one side, it can limit the contact with salts, on the other side, it leads to reduced contact time of the wastewater with the photocatalyst. In fact, the retention time of evaporating water on the active element is short, thus requiring a fast photocatalytic process to ensure optimal purification of the evaporating effluent. To make a simple calculation, if we assume reasonable values for water evaporation rate (1.5 $kg \cdot m^{-2} \cdot h^{-1}$) and pollutant concentration (10 ppm), to fully degrade the pollutant the photocatalyst is supposed to provide a degradation rate of 15 $mg \cdot m^{-2} \cdot h^{-1}$. This is the reason why many systems tested in the literature do not offer a full rejection of the volatile organic pollutant but rather a partial success [151,154]. Other possible solutions to be explored include introducing ionic shielding layers and employing photocatalysts with reduced sensitivity to electrolytes.

These considerations of the device design are not limited to the contact between photocatalyst and salts. Indeed, since the interactions between photothermal and photocatalytic elements are mostly beneficial, it is important to guarantee that such interactions take place; thus, intimate contact between the two photoactive materials shall be obtained. In the majority of works, this is guaranteed either by depositing the photocatalyst on a photothermal material [145,160,167,205]—for instance, on cellulose fibers that are then pyrolyzed to achieve better light capturing—or by producing composite materials where the two are intermixed [35,42,162,175]. The intimate contact between photocatalyst and photothermal element requires a careful materials selection in terms of light absorption properties to maximize solar spectrum utilization. This can be achieved, for instance, by adopting a photocatalytic component absorbing in the UV–visible region and a photothermal catalyst absorbing mainly in the low-energy visible–near infrared (NIR) region [206]. It should be noted, however, that several of the most commonly investigated photothermal materials, such as carbon-based ones, have broad light absorption, which could lower the photocatalytic efficiency by light absorption competition. In this respect, photothermal materials such as noble metal nanoparticles and QDs could offer an advantage due to their highly tunable light absorption properties. Moreover, by engineering suitable heterojunctions, e.g., among high-band-gap photocatalysts like TiO_2 and plasmonic nanoparticles acting as photothermal element, the photocatalytic performances of TiO_2 can be promoted as the noble metal nanoparticles act as electron acceptors when titania is excited with UV light, thus improving charge separation [36,175].

7. Conclusions and Perspectives

This review has examined the potential synergies and incompatibilities between photothermal and photocatalytic materials, highlighting how their interactions, limitations and operating conditions can critically affect solar evaporator performance. Building on this analysis, the main conclusions, together with perspectives and directions for future research, are summarized below.

- The analysis of the current literature indicates that the combination of photothermal and photocatalytic functionalities is indeed a potential benefit for interfacial solar evaporators. While the photocatalyst is not expected to have a negative impact on

the photothermal agent, and vice versa, the added thermal stimulus can support the pollutants degradation action of the photocatalyst thanks to a variety of mechanisms. While the potential synergisms between photocatalysis and thermal catalysis have been investigated in the literature, the interplay between the photocatalyst and the photothermal element in photothermal evaporators has been scarcely explored. The combination of pollutant degradation and rejection by evaporation, the potential occurrence of gas-phase reaction pathways alongside liquid-phase ones, and the possible competition for light absorption between the photocatalyst and the photothermal element all add complexity to the system and require dedicated investigation.

- The analysis of the literature also highlighted a dire need for greater standardization of testing conditions to improve the comparability of results. Moreover, the geometry and materials of the solar still, as well as the testing parameters for photocatalytic and pollutant-rejection experiments, should always be reported. Unfortunately, these aspects are often missing in the literature studies, limiting comparability between different setups.
- Limits to such beneficial interplay mostly come from the materials selection and device configuration, as the choice of where to collocate the two active elements should ensure intimate contact between the two as well as the possibility to effectively convey irradiation at both of their surfaces. In this respect, competition for light absorption should be considered, focusing on strategies to promote charge separation by the formation of Schottky junctions between the photocatalyst and the photothermal material. Along with more commonly employed materials, QDs can represent highly tunable and versatile photothermal materials, allowing them to overcome the risk of light absorption competition.
- Even in the presence of high-quality and highly efficient materials, a non-ideal device configuration can still hamper the overall functionality and its duration over time. The contact time between photocatalyst and pollutant should not be too short (depending on the reaction rate) to guarantee that the process is able to degrade the VOCs contained in water, thus contributing to improvement of the condensed water quality. A higher tortuosity of the porous network containing the photoactive elements can promote reaction rates. In this frame, salt management also plays a vital role: on the one hand, it can negatively affect the photocatalytic performance; on the other, an excess of rejected salts accumulating on the device surface will deactivate both photoactive elements, thus reducing the device lifetime significantly. While possible design strategy and materials choice were discussed here as a function of the type of water effluent to be treated, the literature reports on this topic remain scarce, and further research is urgently needed.

Author Contributions: Conceptualization, D.M., M.V.D. and V.L.; validation, D.M., M.V.D. and V.L.; data curation, H.H. and M.V.D.; writing—original draft preparation, H.H., M.V.D. and V.L.; writing—review and editing, D.M., M.V.D. and V.L.; visualization, D.M., H.H. and M.V.D.; supervision, D.M.; project administration, D.M.; funding acquisition, D.M., M.V.D. and V.L. All authors have read and agreed to the published version of the manuscript.

Funding: This research was funded under the National Recovery and Resilience Plan (NRRP), Mission 4, Component 2, Investment 1.1, Call for tender No. 1409 published on 14 September 2022 by the Italian Ministry of University and Research (MUR), funded by the European Union—NextGenerationEUProject Title COPE—COmposite nanomaterials coupling Photothermal Evaporation and photocatalysis for durable water purification systems—CUP G53D23006660001—Grant Assignment Decree No. 1384 adopted on 1 September 2023 by the Italian Ministry of University and Research (MUR).

Data Availability Statement: No data was produced for this article. All data presented refer to previously published articles.

Acknowledgments: AI (ChatGPT 5.2) was used to draw part of the graphical abstract, specifically, the porous material floating on water under the sun, which was then modified ad adapted by the authors. The technical part of the graphical abstract is not AI-generated.

Conflicts of Interest: The authors declare no conflicts of interest.

References

1. Tao, P.; Ni, G.; Song, C.; Shang, W.; Wu, J.; Zhu, J.; Chen, G.; Deng, T. Solar-Driven Interfacial Evaporation. *Nat. Energy* **2018**, *3*, 1031–1041. [CrossRef]
2. Zhang, Q.; Yao, D.; Gao, X.; Lu, C.; Chen, J.; Wang, W.; Pang, X. Modified PET Fiber Sponge with Synergistic Photothermal Conversion Function for Efficient Solar Interfacial Evaporation. *Desalination* **2026**, *618*, 119502. [CrossRef]
3. Cheng, S.; Sun, C.; Liu, C.; Liu, Y.; Wang, X.; Tan, H.; Li, Y. Titanium Suboxide-Heteropoly Blue Self-Assembled Superlattices for Solar Photothermal High-Efficiency Water Evaporation. *Desalination* **2026**, *617*, 119415. [CrossRef]
4. Zhong, Y.; Zhang, Z.; Tian, J.; Tang, W.; Gao, W.; Li, Y.; Shang, Y. Design of Morphology and Light-Absorbing Tunable FexOy@SiO_2@C Nanoparticles for Solar-Driven Water Evaporation and Purification. *Sep. Purif. Technol.* **2026**, *380*, 135449. [CrossRef]
5. Li, X.; Zhao, H.; Shen, J.; Wen, C.; Luo, L.; Wang, X.; Zheng, R.; Huang, S.; Lin, C.; Sa, B. Self-Assembly Hierarchical MXene/Bacterial Cellulose Composite Films with Accelerated Surface Charge Transfer for Highly Efficient Solar-Driven Water Evaporation. *Sep. Purif. Technol.* **2026**, *382*, 135886. [CrossRef]
6. Fan, X.; Shi, R.; Ahmed, I.; Howells, C.T.; Al Huwayz, M.; Alomar, M.; Shakoor, B.; Shah, M.; Arshad, N.; Ha, V.T.H.; et al. Engineering Interfacial Thermal Energy Management via Grooved B_4C-Polyurethane Architectures for High-Efficiency Solar-Thermal Desalination. *Sep. Purif. Technol.* **2026**, *382*, 135933. [CrossRef]
7. Pan, S.-F.; Liu, W.-X.; Chen, Z.-Y.; Ma, L.; Ding, S.-J.; Wang, Q.-Q. Plasmon-Enhanced Light Absorption and Photothermal Conversion in ReS_2/CoS_2/Cu_2-xS Hollow Nanostructures for Efficient Solar Water Evaporation. *J. Colloid Interface Sci.* **2026**, *704*, 139327. [CrossRef]
8. Cheng, X.; Sun, F.; Yang, L.; Zhou, C.; Liu, C.; Yu, F.; Wang, X.; Zhang, Q. Recent Advanced Optical Adsorption Regulation Strategies in Solar-Driven Evaporation for Efficient Clean Water Production: A Review. *Mater. Res. Bull.* **2024**, *174*, 112730. [CrossRef]
9. Xiao, B.; Zhou, W.; Yu, F.; Wang, J.; Xiong, X.; Liu, G.; Xia, Y.; Wang, X. Materials Design and System Structures of Solar Steam Evaporators. *Environ. Prog. Sustain. Energy* **2023**, *42*, e13944. [CrossRef]
10. Djellabi, R.; Noureen, L.; Dao, V.-D.; Meroni, D.; Falletta, E.; Dionysiou, D.D.; Bianchi, C.L. Recent Advances and Challenges of Emerging Solar-Driven Steam and the Contribution of Photocatalytic Effect. *Chem. Eng. J.* **2022**, *431*, 134024. [CrossRef]
11. Hammoodi, K.A.; Dhahad, H.A.; Alawee, W.H.; Omara, Z.M.; Yusaf, T. Pyramid Solar Distillers: A Comprehensive Review of Recent Techniques. *Results Eng.* **2023**, *18*, 101157. [CrossRef]
12. Abdullah, H.; Shuwanto, H.; Astarini, N.A.; Lie, J.; Ginting, R.T.; Tsai, M.-L.; Shih, S.-J.; Sillanpää, M. A Brief Review of Emerging Strategies in Designing Interfacial Solar Steam Generation for Desalination, Water Purification, Power Generation, and Sea Farming. *ACS Appl. Energy Mater.* **2025**, *8*, 2663–2704. [CrossRef]
13. Mao, K.; Zhang, Y.; Tan, S.C. Functionalizing Solar-Driven Steam Generation towards Water and Energy Sustainability. *Nat. Water* **2025**, *3*, 144–156. [CrossRef]
14. Xu, Y.; Yin, J.; Wang, J.; Wang, X. Design and Optimization of Solar Steam Generation System for Water Purification and Energy Utilization: A Review. *Rev. Adv. Mater. Sci.* **2019**, *58*, 226–247. [CrossRef]
15. Ho, G.W.; Yamauchi, Y.; Hu, L.; Mi, B.; Xu, N.; Zhu, J.; Wang, P. Solar Evaporation and Clean Water. *Nat. Water* **2025**, *3*, 131–134. [CrossRef]
16. Song, C.; Qi, D.; Han, Y.; Xu, Y.; Xu, H.; You, S.; Wang, W.; Wang, C.; Wei, Y.; Ma, J. Volatile-Organic-Compound-Intercepting Solar Distillation Enabled by a Photothermal/Photocatalytic Nanofibrous Membrane with Dual-Scale Pores. *Environ. Sci. Technol.* **2020**, *54*, 9025–9033. [CrossRef]
17. Ma, J.; Xu, Y.; Sun, F.; Chen, X.; Wang, W. Perspective for Removing Volatile Organic Compounds during Solar-Driven Water Evaporation toward Water Production. *EcoMat* **2021**, *3*, e12147. [CrossRef]
18. Iervolino, G.; Zammit, I.; Vaiano, V.; Rizzo, L. Limitations and Prospects for Wastewater Treatment by UV and Visible-Light-Active Heterogeneous Photocatalysis: A Critical Review. In *Heterogeneous Photocatalysis: Recent Advances*; Muñoz-Batista, M.J., Navarrete Muñoz, A., Luque, R., Eds.; Springer International Publishing: Cham, Switzerland, 2020; pp. 225–264.

19. Tucci, A.P.; Murgolo, S.; De Ceglie, C.; Mascolo, G.; Carmagnani, M.; Ronco, P.; Bestetti, M.; Franz, S. Photoelectrocatalytic Advanced Oxidation of Perfluoroalkyl Substances in Groundwaters of the Veneto Region, Italy. *Catal. Today* **2025**, *450*, 115205. [CrossRef]
20. Pérez-Poyatos, L.T.; Pastrana-Martínez, L.M.; Morales-Torres, S.; Maldonado-Hódar, F.J. Novel Strategies to Develop Efficient Carbon/TiO_2 Photocatalysts for the Total Mineralization of VOCs in Air Flows: Improved Synergism between Phases by Mobile N-, O- and S-Functional Groups. *Chem. Eng. J.* **2025**, *508*, 160986. [CrossRef]
21. Xia, M.; Wei, J.; Han, Z.; Tian, Q.; Xiao, C.; Hasi, Q.-M.; Zhang, Y.; Chen, L. An Integrated Solar Absorber with Salt-Resistant and Oleophobic Based on PVDF Composite Membrane for Solar Steam Generation. *Mater. Today Energy* **2022**, *25*, 100959. [CrossRef]
22. Gao, B.; Liu, Z.; Tan, S.H.; Low, S.C. Addressing Critical Challenges of Biofouling in Solar Evaporation: Advanced Strategies for Anti-Biofouling Performance. *Sep. Purif. Technol.* **2025**, *367*, 132874. [CrossRef]
23. Tijing, L.D.; Woo, Y.C.; Choi, J.-S.; Lee, S.; Kim, S.-H.; Shon, H.K. Fouling and Its Control in Membrane Distillation—A Review. *J. Membr. Sci.* **2015**, *475*, 215–244. [CrossRef]
24. Khan, A.; Yadav, S.; Ibrar, I.; Al Juboori, R.A.; Razzak, S.A.; Deka, P.; Subbiah, S.; Shah, S. Fouling and Performance Investigation of Membrane Distillation at Elevated Recoveries for Seawater Desalination and Wastewater Reclamation. *Membranes* **2022**, *12*, 951. [CrossRef] [PubMed]
25. Keller, N.; Ivanez, J.; Highfield, J.; Ruppert, A.M. Photo-/Thermal Synergies in Heterogeneous Catalysis: Towards Low-Temperature (Solar-Driven) Processing for Sustainable Energy and Chemicals. *Appl. Catal. B Environ.* **2021**, *296*, 120320. [CrossRef]
26. Diamanti, M.V.; Shinnur, M.V.; Pedeferri, M.; Ferrari, A.M.; Rosa, R.; Meroni, D. Toward Sustainable Photocatalysis: Addressing Deactivation and Environmental Impact of Anodized and Sol–Gel Photocatalysts. *Adv. Sustain. Syst.* **2025**, *9*, 2401017. [CrossRef]
27. Rimoldi, L.; Meroni, D.; Falletta, E.; Pifferi, V.; Falciola, L.; Cappelletti, G.; Ardizzone, S. Emerging Pollutant Mixture Mineralization by TiO_2 Photocatalysts. The Role of the Water Medium. *Photochem. Photobiol. Sci.* **2017**, *16*, 60–66. [CrossRef]
28. Rioja, N.; Zorita, S.; Peñas, F.J. Effect of Water Matrix on Photocatalytic Degradation and General Kinetic Modeling. *Appl. Catal. B Environ.* **2016**, *180*, 330–335. [CrossRef]
29. Guan, W.; Guo, Y.; Yu, G. Carbon Materials for Solar Water Evaporation and Desalination. *Small* **2021**, *17*, 2007176. [CrossRef]
30. Dao, V.-D.; Choi, H.-S. Carbon-Based Sunlight Absorbers in Solar-Driven Steam Generation Devices. *Glob. Chall.* **2018**, *2*, 1700094. [CrossRef]
31. Meng, T.; Li, Z.; Wan, Z.; Zhang, J.; Wang, L.; Shi, K.; Bu, X.; Alshehri, S.M.; Bando, Y.; Yamauchi, Y.; et al. MOF-Derived Nanoarchitectured Carbons in Wood Sponge Enable Solar-Driven Pumping for High-Efficiency Soil Water Extraction. *Chem. Eng. J.* **2023**, *452*, 139193. [CrossRef]
32. Wei, D.; Wang, C.; Zhang, J.; Zhao, H.; Asakura, Y.; Eguchi, M.; Xu, X.; Yamauchi, Y. Water Activation in Solar-Powered Vapor Generation. *Adv. Mater.* **2023**, *35*, 2212100. [CrossRef] [PubMed]
33. Seh, Z.W.; Liu, S.; Low, M.; Zhang, S.-Y.; Liu, Z.; Mlayah, A.; Han, M.-Y. Janus Au-TiO_2 Photocatalysts with Strong Localization of Plasmonic Near-Fields for Efficient Visible-Light Hydrogen Generation. *Adv. Mater.* **2012**, *24*, 2310–2314. [CrossRef] [PubMed]
34. Wang, C.; Astruc, D. Nanogold Plasmonic Photocatalysis for Organic Synthesis and Clean Energy Conversion. *Chem. Soc. Rev.* **2014**, *43*, 7188–7216. [CrossRef] [PubMed]
35. Huang, J.; He, Y.; Wang, L.; Huang, Y.; Jiang, B. Bifunctional Au@TiO_2 Core–Shell Nanoparticle Films for Clean Water Generation by Photocatalysis and Solar Evaporation. *Energy Convers. Manag.* **2017**, *132*, 452–459. [CrossRef]
36. Stucchi, M.; Meroni, D.; Safran, G.; Villa, A.; Bianchi, C.L.; Prati, L. Noble Metal Promoted TiO_2 from Silver-Waste Valorisation: Synergism between Ag and Au. *Catalysts* **2022**, *12*, 235. [CrossRef]
37. Marelli, M.; Evangelisti, C.; Diamanti, M.V.; Dal Santo, V.; Pedeferri, M.P.; Bianchi, C.L.; Schiavi, L.; Strini, A. TiO_2 Nanotubes Arrays Loaded with Ligand-Free Au Nanoparticles: Enhancement in Photocatalytic Activity. *ACS Appl. Mater. Interfaces* **2016**, *8*, 31051–31058. [CrossRef]
38. Amirjani, A.; Amlashi, N.B.; Ahmadiani, Z.S. Plasmon-Enhanced Photocatalysis Based on Plasmonic Nanoparticles for Energy and Environmental Solutions: A Review. *ACS Appl. Nano Mater.* **2023**, *6*, 9085–9123. [CrossRef]
39. Deeksha, B.; Sadanand, V.; Hariram, N.; Rajulu, A.V. Preparation and Properties of Cellulose Nanocomposite Fabrics with in Situ Generated Silver Nanoparticles by Bioreduction Method. *J. Bioresour. Bioprod.* **2021**, *6*, 75–81. [CrossRef]
40. Gamage McEvoy, J.; Zhang, Z. Antimicrobial and Photocatalytic Disinfection Mechanisms in Silver-Modified Photocatalysts under Dark and Light Conditions. *J. Photochem. Photobiol. C Photochem. Rev.* **2014**, *19*, 62–75. [CrossRef]
41. Shao, Y.; Xu, L.; Sun, M.; Pan, Y.; Lu, X.; Zhao, Y. Fabrication, Photocatalysis and Desalination Properties of 3D MOF/PVDF/MF Evaporator Based on Ag-MOFs. *J. Environ. Chem. Eng.* **2025**, *13*, 116505. [CrossRef]
42. He, X.; Liang, Y.; Li, J.; Lu, Y.; Tian, X.; Wang, Z.; Cao, R.; Ma, P.; Ma, S.; Lu, X. Heterogeneous Structure Based on MXene-TiO_2-Ag with Biomass Hydrogel for Solar Desalination and Photocatalytic Removal of VOCs. *Chem. Eng. J.* **2025**, *523*, 168554. [CrossRef]
43. Song, X.; Wang, Y.; Li, Y.; Jin, X.; Niu, X.; Guo, T.; Zeng, X.; Long, J.; Cheng, G. Enhanced Photothermal Catalytic NO + CO Reaction via Cu/Ce-TiO_2 with Oxygen Vacancies. *Mol. Catal.* **2026**, *588*, 115554. [CrossRef]

44. Yang, Z.; Hou, J.; Guo, J.; Li, Y.; Zhu, Y.; Wan, Y.; Lu, T.; Ding, W. Rational Construction of "All-in-One" Vertically Aligned Copper Single-Atomic Graphene Oxide Based Evaporators for Integrated Solar Steam Generation and Sulfate Radical-Advanced Oxidation Process. *Sep. Purif. Technol.* **2025**, *368*, 132960. [CrossRef]
45. Wang, X.; Wong, K.H.; Yin, Y.; Wang, Z.; Chen, M. Copper-Doped PDA Nanoparticles with Self-Enhanced ROS Generation for Boosting Photothermal/Chemodynamic Combination Therapy. *Biomater. Sci.* **2025**, *13*, 3903–3914. [CrossRef]
46. Ibrahim, I.; Seo, D.H.; McDonagh, A.M.; Shon, H.K.; Tijing, L. Semiconductor Photothermal Materials Enabling Efficient Solar Steam Generation toward Desalination and Wastewater Treatment. *Desalination* **2021**, *500*, 114853. [CrossRef]
47. Tao, F.; Zhang, Y.; Cao, S.; Yin, K.; Chang, X.; Lei, Y.; Fan, R.; Dong, L.; Yin, Y.; Chen, X. CuS Nanoflowers/Semipermeable Collodion Membrane Composite for High-Efficiency Solar Vapor Generation. *Mater. Today Energy* **2018**, *9*, 285–294. [CrossRef]
48. Zhao, Y.; Pan, H.; Lou, Y.; Qiu, X.; Zhu, J.; Burda, C. Plasmonic $Cu_{2-x}S$ Nanocrystals: Optical and Structural Properties of Copper-Deficient Copper(I) Sulfides. *J. Am. Chem. Soc.* **2009**, *131*, 4253–4261. [CrossRef]
49. Coughlan, C.; Ibáñez, M.; Dobrozhan, O.; Singh, A.; Cabot, A.; Ryan, K.M. Compound Copper Chalcogenide Nanocrystals. *Chem. Rev.* **2017**, *117*, 5865–6109. [CrossRef]
50. Seifikar, F.; Habibi-Yangjeh, A.; Jahed-Jaafargolikhanlo, M. A Critical Review on Emerging Photothermal-Photocatalytic Materials Composed of g-C_3N_4 for Energy Production and Environmental Remediation. *J. Environ. Chem. Eng.* **2025**, *13*, 115812. [CrossRef]
51. Bhanderi, D.; Lakhani, P.; Modi, C.K. Graphitic Carbon Nitride (g-C_3N_4) as an Emerging Photocatalyst for Sustainable Environmental Applications: A Comprehensive Review. *RSC Sustain.* **2024**, *2*, 265–287. [CrossRef]
52. da Rosa Cunha, G.; Guaglianoni, W.C.; Bergmann, C.P. CNT/TiO_2 Hybrid Nanostructured Materials: Synthesis, Properties and Applications. In *Environmental Applications of Nanomaterials*; Kopp Alves, A., Ed.; Springer International Publishing: Cham, Switzerland, 2022; pp. 185–204.
53. Vijayan, B.K.; Dimitrijevic, N.M.; Finkelstein-Shapiro, D.; Wu, J.; Gray, K.A. Coupling Titania Nanotubes and Carbon Nanotubes to Create Photocatalytic Nanocomposites. *ACS Catal.* **2012**, *2*, 223–229. [CrossRef]
54. Xin, W.; Xiao, H.; Kong, X.-Y.; Chen, J.; Yang, L.; Niu, B.; Qian, Y.; Teng, Y.; Jiang, L.; Wen, L. Biomimetic Nacre-Like Silk-Crosslinked Membranes for Osmotic Energy Harvesting. *ACS Nano* **2020**, *14*, 9701–9710. [CrossRef]
55. Zhai, Z.; Dong, X.; Qi, H.; Tao, R.; Zhang, P. Carbon Quantum Dots with High Photothermal Conversion Efficiency and Their Application in Photothermal Modulated Reversible Deformation of Poly(N-Isopropylacrylamide) Hydrogel. *ACS Appl. Bio Mater.* **2023**, *6*, 3395–3405. [CrossRef] [PubMed]
56. Jiang, T.; Guo, C.; Qian, S.; Wang, J.; Zhu, K.; Xue, H.; Tian, J. Self-Assembly of Graphene Quantum Dots into High-Aspect-Ratio Carbon Fibers for Effective Solar Water Desalination. *Sep. Purif. Technol.* **2025**, *371*, 133378. [CrossRef]
57. Slejko, E.A.; Sayevich, V.; Cai, B.; Gaponik, N.; Lughi, V.; Lesnyak, V.; Eychmu, A. Precise Engineering of Nanocrystal Shells via Colloidal Atomic Layer Deposition. *Chem. Mater.* **2017**, *29*, 8111–8118. [CrossRef]
58. Bruner, L.; Kozak, J. Zur Kenntnis Der Photokatalyse. I. Die Lichtreaktion in Gemischen: Uransalz + Oxalsäure. *Z. Elektrochem. Angew. Phys. Chem.* **1911**, *17*, 354–360. [CrossRef]
59. Eibner, A. Action of Light on Pigments. *Chemiker-Zeitung* **1911**, *35*, 753–755.
60. Hashimoto, K.; Irie, H.; Fujishima, A. TiO_2 Photocatalysis: A Historical Overview and Future Prospects. *Jpn. J. Appl. Phys.* **2005**, *44*, 8269. [CrossRef]
61. Guillard, C.; Robert, D. Fifty Years of Research in Environmental Photocatalysis: Scientific Advances, Discoveries, and New Perspectives. *Catalysts* **2024**, *14*, 547. [CrossRef]
62. Sordello, F.; Calza, P.; Minero, C.; Malato, S.; Minella, M. More than One Century of History for Photocatalysis, from Past, Present and Future Perspectives. *Catalysts* **2022**, *12*, 1572. [CrossRef]
63. Goodeve, C.F.; Kitchener, J.A. Photosensitisation by Titanium Dioxide. *Trans. Faraday Soc.* **1938**, *34*, 570–579. [CrossRef]
64. Fujishima, A.; Honda, K. Electrochemical Photolysis of Water at a Semiconductor Electrode. *Nature* **1972**, *238*, 37–38. [CrossRef] [PubMed]
65. Parrino, F.; D'Arienzo, M.; Mostoni, S.; Dirè, S.; Ceccato, R.; Bellardita, M.; Palmisano, L. Electron and Energy Transfer Mechanisms: The Double Nature of TiO_2 Heterogeneous Photocatalysis. *Top. Curr. Chem.* **2021**, *380*, 2. [CrossRef] [PubMed]
66. Carp, O.; Huisman, C.L.; Reller, A. Photoinduced Reactivity of Titanium Dioxide. *Prog. Solid State Chem.* **2004**, *32*, 33–177. [CrossRef]
67. Chakravorty, A.; Roy, S. A Review of Photocatalysis, Basic Principles, Processes, and Materials. *Sustain. Chem. Environ.* **2024**, *8*, 100155. [CrossRef]
68. Augugliaro, V.; Bellardita, M.; Loddo, V.; Palmisano, G.; Palmisano, L.; Yurdakal, S. Overview on Oxidation Mechanisms of Organic Compounds by TiO_2 in Heterogeneous Photocatalysis. *J. Photochem. Photobiol. C Photochem. Rev.* **2012**, *13*, 224–245. [CrossRef]
69. Zhu, S.; Wang, D. Photocatalysis: Basic Principles, Diverse Forms of Implementations and Emerging Scientific Opportunities. *Adv. Energy Mater.* **2017**, *7*, 1700841. [CrossRef]
70. Mills, A.; Le Hunte, S. An Overview of Semiconductor Photocatalysis. *J. Photochem. Photobiol. Chem.* **1997**, *108*, 1–35. [CrossRef]

71. Wafi, A.; Aji, D.; Khan, M.M. Recent Advances in Photocatalysis: From Laboratory to Market. *Results Chem.* **2025**, *18*, 102672. [CrossRef]
72. Diamanti, M.V.; Pedeferri, M. Concrete, Mortar and Plaster Using Titanium Dioxide Nanoparticles: Applications in Pollution Control, Self-Cleaning and Photo Sterilization. In *Nanotechnology in Eco-Efficient Construction*; Elsevier: Amsterdam, The Netherlands, 2013; pp. 299–326.
73. Jenima, J.; Priya Dharshini, M.; Ajin, M.L.; Jebeen Moses, J.; Retnam, K.P.; Arunachalam, K.P.; Avudaiappan, S.; Arrue Munoz, R.F. A Comprehensive Review of Titanium Dioxide Nanoparticles in Cementitious Composites. *Heliyon* **2024**, *10*, e39238. [CrossRef]
74. Jadhav, A.J.; Goswami, A.D.; Trivedi, D.H.; Chavan, P.V.; Jadhav, N.L.; Pinjari, D.V. A Comprehensive Review on Pure and Doped Titanium Oxide Nanoparticles for Photocatalytic Applications. *Inorg. Chem. Commun.* **2025**, *181*, 115206. [CrossRef]
75. Gupta, S.M.; Tripathi, M. A Review of TiO_2 Nanoparticles. *Chin. Sci. Bull.* **2011**, *56*, 1639–1657. [CrossRef]
76. Hosseini, F.; Assadi, A.A.; Nguyen-Tri, P.; Ali, I.; Rtimi, S. Titanium-Based Photocatalytic Coatings for Bacterial Disinfection: The Shift from Suspended Powders to Catalytic Interfaces. *Surf. Interfaces* **2022**, *32*, 102078. [CrossRef]
77. Obregón, S.; Rodríguez-González, V. Photocatalytic TiO_2 Thin Films and Coatings Prepared by Sol–Gel Processing: A Brief Review. *J. Sol-Gel Sci. Technol.* **2022**, *102*, 125–141. [CrossRef]
78. Mulus, D.A.S.; Permana, M.D.; Deawati, Y.; Eddy, D.R. A Current Review of TiO_2 Thin Films: Synthesis and Modification Effect to the Mechanism and Photocatalytic Activity. *Appl. Surf. Sci. Adv.* **2025**, *27*, 100746. [CrossRef]
79. Xu, Y.; Chiam, S.L.; Leo, C.P.; Hu, Z. Recent Advances in Photocatalytic TiO_2-Based Membranes for Eliminating Water Pollutants. *Sep. Purif. Rev.* **2025**, 1–18. [CrossRef]
80. Covaliu-Mierlă, C.I.; Matei, E.; Stoian, O.; Covaliu, L.; Constandache, A.-C.; Iovu, H.; Paraschiv, G. TiO_2–Based Nanofibrous Membranes for Environmental Protection. *Membranes* **2022**, *12*, 236. [CrossRef]
81. Szaniawska-Białas, E.; Brudzisz, A.; Nasir, A.; Wierzbicka, E. Recent Advances in Preparation, Modification, and Application of Free-Standing and Flow-Through Anodic TiO_2 Nanotube Membranes. *Molecules* **2024**, *29*, 5638. [CrossRef]
82. Vaccari, M.; Orsi, D.; Cristofolini, L. Tailoring Solid Foam Structures for High-Efficiency Photocatalytic Filtration of Air and Water. *Mater. Des.* **2025**, *260*, 114980. [CrossRef]
83. Isley, S.L.; Penn, R.L. Titanium Dioxide Nanoparticles: Effect of Sol-Gel pH on Phase Composition, Particle Size, and Particle Growth Mechanism. *J. Phys. Chem. C* **2008**, *112*, 4469–4474. [CrossRef]
84. Kim, S.-W.; Hou, Y.; Madhan, K.; Senthilkumar, K.; Kim, H.-S.; Kim, W.-J. Sol-Gel Nano TiO_2 Synthesis Using TTIP: Latest Trends, a Comprehensive Review of Attribute Optimization and Various Applications. *Mater. Today* **2025**, *88*, 457–478. [CrossRef]
85. Kovalenko, D.; Gaishun, V.; Vaskevich, V.; Semchenko, A.; Ruzimuradov, O. TiO_2 Sol–Gel Nanomaterials: Synthesis, Properties and Applications. In *Titanium Dioxide-Based Multifunctional Hybrid Nanomaterials: Application on Health, Energy and Environment*; Prakash, J., Cho, J., Ruzimuradov, O., Fang, D., Eds.; Springer Nature: Cham, Switzerland, 2025; pp. 55–72.
86. Wang, Y.-H.; Rahman, K.H.; Wu, C.-C.; Chen, K.-C. A Review on the Pathways of the Improved Structural Characteristics and Photocatalytic Performance of Titanium Dioxide (TiO_2) Thin Films Fabricated by the Magnetron-Sputtering Technique. *Catalysts* **2020**, *10*, 598. [CrossRef]
87. Vahl, A.; Veziroglu, S.; Henkel, B.; Strunskus, T.; Polonskyi, O.; Aktas, O.C.; Faupel, F. Pathways to Tailor Photocatalytic Performance of TiO_2 Thin Films Deposited by Reactive Magnetron Sputtering. *Materials* **2019**, *12*, 2840. [CrossRef] [PubMed]
88. Santos, J.S.; Sikora, M.S.; Trivinho-Strixino, F.; Praserthdam, S.; Praserthdam, P. A Comprehensive Review of Anodic TiO_2 Films as Heterogeneous Catalysts for Photocatalytic and Photoelectrocatalytic Water Disinfection. *J. Water Process Eng.* **2025**, *69*, 106589. [CrossRef]
89. Boykobilov, D.; Thakur, S.; Samiev, A.; Nasimov, A.; Turaev, K.; Nurmanov, S.; Prakash, J.; Ruzimuradov, O. Electrochemical Synthesis and Modification of Novel TiO_2 Nanotubes: Chemistry and Role of Key Synthesis Parameters for Photocatalytic Applications in Energy and Environment. *Inorg. Chem. Commun.* **2024**, *170*, 113419. [CrossRef]
90. Kowalski, D.; Kim, D.; Schmuki, P. TiO_2 Nanotubes, Nanochannels and Mesosponge: Self-Organized Formation and Applications. *Nano Today* **2013**, *8*, 235–264. [CrossRef]
91. Shinnur, M.V.; Pedeferri, M.; Diamanti, M.V. Properties and Photocatalytic Applications of Black TiO_2 Produced by Thermal or Plasma Hydrogenation. *Curr. Res. Green Sustain. Chem.* **2024**, *8*, 100415. [CrossRef]
92. Slapničar, Š.; Caf, M.; Kralj, S.; Žerjav, G.; Pintar, A. Revealing the Dual Role of Nanoparticle Size and Surface Ligands in Plasmon-Enhanced Photocatalysis of Au/TiO_2 Nanorods. *Appl. Surf. Sci.* **2026**, *720*, 165300. [CrossRef]
93. Selishchev, D.; Lyulyukin, M.; Polskikh, D.; Kovalevskaya, K.; Selishcheva, S.; Cherepanova, S.; Gerasimov, E.; Bukhtiyarov, A.; Li, Y.; Zhang, G. Fe-Decorated Bi_2WO_6/TiO_2-N Heterostructure Photocatalyst for Enhanced Visible Light-Driven Degradation of Organic Micropollutants in Air. *Sep. Purif. Technol.* **2026**, *380*, 135146. [CrossRef]
94. Pérez-Poyatos, L.T.; Morales-Torres, S.; Pastrana-Martínez, L.M.; Maldonado-Hódar, F.J. Sulfur-Doped Carbon/TiO_2 Composites for Ethylene Photo-Oxidation. Enhanced Performance by Doping TiO_2 Phases with Sulfur by Mobile Species Inserted on the Carbon Support. *Catal. Today* **2025**, *446*, 115115. [CrossRef]

95. Chen, X.; Liu, L.; Yu, P.Y.; Mao, S.S. Increasing Solar Absorption for Photocatalysis with Black Hydrogenated Titanium Dioxide Nanocrystals. *Science* **2011**, *331*, 746–750. [CrossRef] [PubMed]
96. Vanlalhmingmawia, C.; Lee, S.M.; Tiwari, D. Plasmonic Noble Metal Doped Titanium Dioxide Nanocomposites: Newer and Exciting Materials in the Remediation of Water Contaminated with Micropollutants. *J. Water Process Eng.* **2023**, *51*, 103360. [CrossRef]
97. Sharma, A.K.; Choudhary, H.; Chauhan, P.; Chaliha, J. Nanomaterials for the Remediation of Microplastics in Wastewater. *Nano Trends* **2025**, *12*, 100152. [CrossRef]
98. Ruiz-Castillo, A.L.; Hinojosa-Reyes, M.; Camposeco, R.; Hinojosa-Reyes, L. Advances in Bi_2O_3-Based Photocatalysts: A Review on Synergistic Modifications and Wastewater Treatment Applications. *Inorg. Chem. Commun.* **2026**, *183*, 115730. [CrossRef]
99. Baig, A.; Siddique, M.; Panchal, S. A Review of Visible-Light-Active Zinc Oxide Photocatalysts for Environmental Application. *Catalysts* **2025**, *15*, 100. [CrossRef]
100. Chiam, S.-L.; Pung, S.-Y.; Yeoh, F.-Y. Recent Developments in MnO_2-Based Photocatalysts for Organic Dye Removal: A Review. *Environ. Sci. Pollut. Res.* **2020**, *27*, 5759–5778. [CrossRef]
101. Chirkunova, N.; Azaizia, A.; Domarev, S.; Dorogov, M. Nanostructured Copper Oxide Materials for Photocatalysis and Sensors. *Eng. Proc.* **2025**, *118*, 16. [CrossRef]
102. Zindrou, A.; Belles, L.; Deligiannakis, Y. Cu-Based Materials as Photocatalysts for Solar Light Artificial Photosynthesis: Aspects of Engineering Performance, Stability, Selectivity. *Solar* **2023**, *3*, 87–112. [CrossRef]
103. Zeng, S.; Si, J.; Cui, Z.; Yuan, Z. Metal-Organic Framework-Based Materials for Solar-Driven Interfacial Evaporation. *Chem. Eng. J.* **2024**, *502*, 158111. [CrossRef]
104. Yue, C.; Chen, L.; Zhang, H.; Huang, J.; Jiang, H.; Li, H.; Yang, S. Metal–Organic Framework-Based Materials: Emerging High-Efficiency Catalysts for the Heterogeneous Photocatalytic Degradation of Pollutants in Water. *Environ. Sci. Water Res. Technol.* **2023**, *9*, 669–695. [CrossRef]
105. El Messaoudi, N.; Ciğeroğlu, Z.; Şenol, Z.M.; Elhajam, M.; Noureen, L. A Comparative Review of the Adsorption and Photocatalytic Degradation of Tetracycline in Aquatic Environment by G-C_3N_4-Based Materials. *J. Water Process Eng.* **2023**, *55*, 104150. [CrossRef]
106. Rout, D.R.; Jena, H.M.; Kumar, A.; Baigenzhenov, O.; Hosseini-Bandegharaei, A. Graphene-, GO-, and rGO-Supported Photocatalysts for Degradation of Organic Pollutants: A Comprehensive Review. *Environ. Technol. Innov.* **2025**, *40*, 104560. [CrossRef]
107. Zondag, S.D.A.; Mazzarella, D.; Noël, T. Scale-Up of Photochemical Reactions: Transitioning from Lab Scale to Industrial Production. *Annu. Rev. Chem. Biomol. Eng.* **2023**, *14*, 283–300. [CrossRef] [PubMed]
108. Alalm, M.G.; Djellabi, R.; Meroni, D.; Pirola, C.; Bianchi, C.L.; Boffito, D.C. Toward Scaling-Up Photocatalytic Process for Multiphase Environmental Applications. *Catalysts* **2021**, *11*, 562. [CrossRef]
109. Samer, M. Biological and Chemical Wastewater Treatment Processes. In *Wastewater Treatment Engineering*; Samer, M., Ed.; IntechOpen: London, UK, 2015.
110. Cozzolino, V.; Coppola, G.; Calabrò, V.; Chakraborty, S.; Candamano, S.; Algieri, C. Heterogeneous TiO_2 Photocatalysis Coupled with Membrane Technology for Persistent Contaminant Degradation: A Critical Review. *Appl. Water Sci.* **2025**, *15*, 243. [CrossRef]
111. Kayahan, E.; Jacobs, M.; Braeken, L.; Thomassen, L.C.; Kuhn, S.; van Gerven, T.; Leblebici, M.E. Dawn of a New Era in Industrial Photochemistry: The Scale-up of Micro- and Mesostructured Photoreactors. *Beilstein J. Org. Chem.* **2020**, *16*, 2484–2504. [CrossRef]
112. Buglioni, L.; Raymenants, F.; Slattery, A.; Zondag, S.D.A.; Noël, T. Technological Innovations in Photochemistry for Organic Synthesis: Flow Chemistry, High-Throughput Experimentation, Scale-up, and Photoelectrochemistry. *Chem. Rev.* **2022**, *122*, 2752–2906. [CrossRef]
113. Wen, Z.; Pintossi, D.; Nuño, M.; Noël, T. Membrane-Based TBADT Recovery as a Strategy to Increase the Sustainability of Continuous-Flow Photocatalytic HAT Transformations. *Nat. Commun.* **2022**, *13*, 6147. [CrossRef]
114. Majumder, A.; Otter, P.; Röher, D.; Bhatnagar, A.; Khalil, N.; Gupta, A.K.; Bresciani, R.; Arias, C.A. Combination of Advanced Biological Systems and Photocatalysis for the Treatment of Real Hospital Wastewater Spiked with Carbamazepine: A Pilot-Scale Study. *J. Environ. Manag.* **2024**, *351*, 119672. [CrossRef]
115. Goel, M.; Joshi, N.; Verma, A. Scaled-Up Sustainable Wastewater Treatment of Tertiary Effluent for the Removal of Chromophores Using Dual Advanced Oxidation Processes. *Environ. Qual. Manag.* **2025**, *35*, e70204. [CrossRef]
116. Kubiak, A. A Scalable IoT-Controlled Photocatalytic System for Pharmaceutical Removal in Real Wastewater Treatment Applications. *Chem. Eng. J.* **2025**, *518*, 164709. [CrossRef]
117. Zhao, W.; Chen, I.-W.; Huang, F. Toward Large-Scale Water Treatment Using Nanomaterials. *Nano Today* **2019**, *27*, 11–27. [CrossRef]
118. Sioulas, S.; Rapti, I.; Kosma, C.; Konstantinou, I.; Albanis, T. Photocatalytic Degradation of the Antidepressant Drug Paroxetine Using TiO_2 P-25 under Lab and Pilot Scales in Aqueous Substrates. *Water Emerg. Contam. Nanoplast.* **2025**, *4*, 5. [CrossRef]

119. Castro-Rojas, J.; Rao, M.A.; Berruti, I.; Mora, M.L.; Garrido-Ramírez, E.; Polo-López, M.I. Assessment of Solar Photocatalytic Wastewater Disinfection and Microcontaminants Removal by Modified-Allophane Nanoclays Based on TiO_2, Fe and ZnO at Laboratory and Pilot Scale. *Chem. Eng. J.* **2025**, *503*, 157894. [CrossRef]
120. Rapti, I.; Kosma, C.; Albanis, T.; Konstantinou, I. Solar Photocatalytic Degradation of Inherent Pharmaceutical Residues in Real Hospital WWTP Effluents Using Titanium Dioxide on a CPC Pilot Scale Reactor. *Catal. Today* **2023**, *423*, 113884. [CrossRef]
121. Li, X.; Everitt, H.O.; Liu, J. Synergy between Thermal and Nonthermal Effects in Plasmonic Photocatalysis. *Nano Res.* **2020**, *13*, 1268–1280. [CrossRef]
122. Sun, M.; Zhao, B.; Chen, F.; Liu, C.; Lu, S.; Yu, Y.; Zhang, B. Thermally-Assisted Photocatalytic CO_2 Reduction to Fuels. *Chem. Eng. J.* **2021**, *408*, 127280. [CrossRef]
123. Li, X.; Wang, W.; Dong, F.; Zhang, Z.; Han, L.; Luo, X.; Huang, J.; Feng, Z.; Chen, Z.; Jia, G.; et al. Recent Advances in Noncontact External-Field-Assisted Photocatalysis: From Fundamentals to Applications. *ACS Catal.* **2021**, *11*, 4739–4769. [CrossRef]
124. Ye, X.; Zeng, W.; Guan, X.; Zhang, T.; Guo, L. Green Energy and Chemicals from Biomass via Thermo-Photo Catalysis: Fundamentals, Progress, and Opportunities. *Coord. Chem. Rev.* **2026**, *546*, 217041. [CrossRef]
125. Fang, S.; Sun, Z.; Hu, Y.H. Insights into the Thermo-Photo Catalytic Production of Hydrogen from Water on a Low-Cost NiOx-Loaded TiO_2 Catalyst. *ACS Catal.* **2019**, *9*, 5047–5056. [CrossRef]
126. Castedo, A.; Casanovas, A.; Angurell, I.; Soler, L.; Llorca, J. Effect of Temperature on the Gas-Phase Photocatalytic H_2 Generation Using Microreactors under UVA and Sunlight Irradiation. *Fuel* **2018**, *222*, 327–333. [CrossRef]
127. Highfield, J.G.; Chen, M.H.; Nguyen, P.T.; Chen, Z. Mechanistic Investigations of Photo-Driven Processes over TiO_2 by in-Situ DRIFTS-MS: Part 1. Platinization and Methanol Reforming. *Energy Environ. Sci.* **2009**, *2*, 991–1002. [CrossRef]
128. Nikitenko, S.I.; Chave, T.; Cau, C.; Brau, H.-P.; Flaud, V. Photothermal Hydrogen Production Using Noble-Metal-Free Ti@TiO_2 Core–Shell Nanoparticles under Visible–NIR Light Irradiation. *ACS Catal.* **2015**, *5*, 4790–4795. [CrossRef]
129. Ye, L.; Chu, K.H.; Wang, B.; Wu, D.; Xie, H.; Huang, G.; Yip, H.Y.; Wong, P.K. Noble-Metal Loading Reverses Temperature Dependent Photocatalytic Hydrogen Generation in Methanol–Water Solutions. *Chem. Commun.* **2016**, *52*, 11657–11660. [CrossRef]
130. Han, X.; Song, L.; Xu, H.; Ouyang, S. Light-Driven Low-Temperature Syngas Production from CH_3OH and H_2O over a Pt@$SrTiO_3$ Photothermal Catalyst. *Catal. Sci. Technol.* **2018**, *8*, 2515–2518. [CrossRef]
131. Xu, S.; Zhu, W.; Wu, L.; Zhang, X.; Li, C.; Wang, Y.; Yang, Y. Pyro-Photocatalytic Coupled Effect in Ferroelectric $Bi_{0.5}Na_{0.5}TiO_3$ Nanoparticles for Enhanced Dye Degradation. *ACS Appl. Mater. Interfaces* **2023**, *15*, 1276–1285. [CrossRef]
132. Bhatt, V.; Choi, M.-J. Recent Progress in Pyro-Phototronic Effect-Based Photodetectors: A Path Toward Next-Generation Optoelectronics. *Materials* **2025**, *18*, 976. [CrossRef]
133. Dai, B.; Gao, C.; Guo, J.; Ding, M.; Xu, Q.; He, S.; Mou, Y.; Dong, H.; Hu, M.; Dai, Z.; et al. A Robust Pyro-Phototronic Route to Markedly Enhanced Photocatalytic Disinfection. *Nano Lett.* **2024**, *24*, 4816–4825. [CrossRef]
134. Djellabi, R.; Rtimi, S. Unleashing Photothermocatalysis Potential for Enhanced Pathogenic Bacteria Inactivation. *Chem. Eng. J.* **2025**, *506*, 159976. [CrossRef]
135. Li, W.; Lv, G.; Liu, M.; Zhao, F.; Shuai, P.; Feng, Y.; Chen, D.; Liao, L. Photothermal-Driven Enhancing Photocatalysis and Photoelectrocatalysis: Advances and Perspectives. *J. Energy Chem.* **2025**, *108*, 332–360. [CrossRef]
136. Villar-Chavero, M.M.; Domínguez, J.C.; Alonso, M.V.; Oliet, M.; Rodriguez, F. Thermal and Kinetics of the Degradation of Chitosan with Different Deacetylation Degrees under Oxidizing Atmosphere. *Thermochim. Acta* **2018**, *670*, 18–26. [CrossRef]
137. Chen, Z.; Kuate, L.J.N.; Zhang, H.; Hou, J.; Wen, H.; Lu, C.; Li, C.; Shi, W. Photothermally Enabled Black G-C_3N_4 Hydrogel with Integrated Solar-Driven Evaporation and Photo-Degradation for Efficient Water Purification. *Sep. Purif. Technol.* **2025**, *355*, 129751. [CrossRef]
138. Wang, P.; Yuan, Q. Synergistic Experimental Study by a Solar Pilot Evaporation System for the Volume Reduction and Antibiotics Photocatalytic Degradation of Liquid Digestate. *J. Water Process Eng.* **2024**, *59*, 105023. [CrossRef]
139. Sajjadizadeh, H.-S.; Goharshadi, E.K.; Karimi-Nazarabad, M. An Efficient Monolithic Green Reactor for Photo(Electro)Catalysis: Hybridizing g-C_3N_4 with Fe/Ni Nanoparticles on Wood Sponge for Water Oxidation, N_2 and CO_2 Photofixation, and Interfacial Solar Steam Generation. *Renew. Energy* **2026**, *256*, 124068. [CrossRef]
140. Tang, Q.; Zhang, Z.; Pan, Y.; Leung, M.K.H.; Zhang, Y.; Chen, K. Carbon Nitride Gels: Synthesis, Modification, and Water Decontamination Applications. *Gels* **2025**, *11*, 685. [CrossRef]
141. Zhou, Q.; Chen, Y.; Wang, D.; Yang, W.; Su, Z. Mof-Based Hydrogels with Photothermal and Photocatalytic Activity for Efficient Solar Water Evaporation and Purification. *Chem. Eng. Sci.* **2026**, *320*, 122491. [CrossRef]
142. An, N.; Ma, M.; Chen, Y.; Wang, Z.; Li, Q. Biomass Hydrogel Solar-Driven Multifunctional Evaporator for Desalination, VOC Removal, and Sterilization. *ACS EST Eng.* **2025**, *5*, 732–742. [CrossRef]
143. Zhu, H.; Xu, Z.; Xiao, M.; Zhao, D.; Wang, Q.; Fu, Y.; Zhu, J.; Xiong, X.; Jiang, R. Multifunctional and Sustainable Chitosan-Based Interfacial Materials for Effective Water Evaporation, Desalination, and Wastewater Purification: A Review. *Int. J. Biol. Macromol.* **2025**, *321*, 145973. [CrossRef]

144. Ye, M.; Xing, H.; You, Y.; Xie, Y.; Liu, Y.; Chu, W.; Zhang, A.; Lin, X.; Xue, J.; Lu, Y. Bioinspired Unidirectional 3D Scaffold for Synergistic Enhanced Solar Evaporation and Efficient VOCs Degradation. *Small* **2025**, *21*, 2501729. [CrossRef]
145. Liu, Y.; Lou, J.; Ni, M.; Song, C.; Wu, J.; Dasgupta, N.P.; Tao, P.; Shang, W.; Deng, T. Bioinspired Bifunctional Membrane for Efficient Clean Water Generation. *ACS Appl. Mater. Interfaces* **2016**, *8*, 772–779. [CrossRef]
146. Wang, X.; He, Y.; Liu, X. Synchronous Steam Generation and Photodegradation for Clean Water Generation Based on Localized Solar Energy Harvesting. *Energy Convers. Manag.* **2018**, *173*, 158–166. [CrossRef]
147. Tian, Y.; Yang, H.; Wu, S.; Gong, B.; Xu, C.; Yan, J.; Cen, K.; Bo, Z.; Ostrikov, K. High-performance Water Purification and Desalination by Solar-driven Interfacial Evaporation and Photocatalytic VOC Decomposition Enabled by Hierarchical TiO_2–CuO Nanoarchitecture. *Int. J. Energy Res.* **2022**, *46*, 1313–1326. [CrossRef]
148. Wang, W.; Yao, D.; Gao, X.; Lu, C.; Chen, J.; Zhang, Q.; Pang, X. Bio-Based Sponge-like Porous Hydrogels via Cryo-Polymerization for Efficient Solar Interfacial Evaporation. *Chem. Eng. J.* **2025**, *522*, 167670. [CrossRef]
149. Hu, B.; Shu, D.; Zhou, Y.; Fan, L.; Bai, Z.; Ye, D.; Xu, J. Cellulose Nanofiber-Based Aerogel with Janus Wettability for Superior Evaporation Performance and Synergistic Photocatalytic Activities. *Carbohydr. Polym.* **2025**, *368*, 124166. [CrossRef]
150. Zhang, B.; Wu, W.; Yin, G.; Gong, X. A Multifunctional Synergistic Solar-Driven Interfacial Evaporator for Desalination and Photocatalytic Degradation. *ACS Appl. Mater. Interfaces* **2025**, *17*, 6948–6956. [CrossRef]
151. Deng, J.; Xiao, S.; Wang, B.; Li, Q.; Li, G.; Zhang, D.; Li, H. Self-Suspended Photothermal Microreactor for Water Desalination and Integrated Volatile Organic Compound Removal. *ACS Appl. Mater. Interfaces* **2020**, *12*, 51537–51545. [CrossRef]
152. Ren, L.; Yang, X.; Sun, X.; Yuan, Y. Synchronizing Efficient Purification of VOCs in Durable Solar Water Evaporation over a Highly Stable Cu/$W_{18}O_{49}$@Graphene Material. *Nano Lett.* **2024**, *24*, 715–723. [CrossRef]
153. Ma, C.; An, X.; Guo, M. A Wood-Based Evaporator with Robust Photothermal Layer Enabling Efficient Solar Evaporation and Antibiotic Photodegradation. *Water Res.* **2025**, *285*, 124129. [CrossRef]
154. Shi, C.; Zhang, J.; Wu, P.; Xia, M.; Jiang, Q.; Yang, X.; Shi, Y.; Owens, G.; Pi, K. An Integrated Photothermal–Photocatalytic Strategy for in Situ Treatment and Water Reuse of Landfill Leachate. *J. Hazard. Mater.* **2025**, *498*, 139914. [CrossRef]
155. An, N.; Zhang, X.; Chen, Y.; Wang, Z.; Qiu, J.; Gao, B.; Li, Q. A Self-Floating Photothermal/Photocatalytic Evaporator for Simultaneous High-Efficiency Evaporation and Purification of Volatile Organic Wastewater. *Adv. Funct. Mater.* **2025**, *35*, 2500777. [CrossRef]
156. Yang, Y.; Ya, Y.; Li, J.; Lai, J.; Liu, C. Plant Stem-Inspired Biomimetic Design of Hydrogel Skin-Fiber Bundle Evaporator for Dynamic Solar Treatment and Resource Re-Utilization of High-Salinity Dye Wastewater. *Chem. Eng. J.* **2025**, *522*, 167461. [CrossRef]
157. Xu, X.; Qiu, J.; Li, Z.; Fu, A.; Yuan, S.; Li, H.; Lu, B. A Bifunctional Polyacrylamide-Alginate-TiO_2 Hydrogel Solar Evaporator for Integrated High-Efficiency Desalination and Photocatalytic Degradation. *Desalination* **2025**, *611*, 118920. [CrossRef]
158. Zhu, C.; Xiao, X.; Wang, X.; Ma, Z.; Han, Y. Sodium Alginate/TiO_2 Bilayer Material Multiphase Photocatalytic Degradation of Seawater Pollutants and Synergistic Seawater Evaporation. *ACS Appl. Nano Mater.* **2024**, *7*, 27287–27298. [CrossRef]
159. Xu, X.; Liu, Q.; Qiu, J.; Zhao, Q.; Yuan, S.; Li, H.; Li, Z.; Fu, A.; Xu, J.; Lu, B. Photothermal-Photocatalytic Bifunctional Highly Porous Hydrogel for Efficient Coherent Sewage Purification-Clean Water Generation. *Desalination* **2025**, *597*, 118364. [CrossRef]
160. Wang, K.; Li, W.; Long, Y. Bifunctional N-TiO_2/C/PU Foam for Interfacial Water Evaporation and Sewage Purification. *Materials* **2025**, *18*, 1550. [CrossRef]
161. Dong, S.; Li, X.; Zhang, J.; Hu, Y.; Yan, C.; Wang, S.; Gao, Y. N-Doped Fe_3O_4 Nanoparticles Loaded-Carbon Foam for a Highly Efficient and Recyclable Desalination-Photocatalysis Solar Evaporator. *Sep. Purif. Technol.* **2025**, *361*, 131425. [CrossRef]
162. Du, Y.; Yang, X.; Wu, T.; Chen, Y.; Xie, H.; Wang, S.; Chang, Z. Antibacterial and Photocatalytic PVDF Foam for Simultaneous Interface Evaporation and Water Purification. *J. Mater. Sci. Technol.* **2026**, *248*, 99–109. [CrossRef]
163. Yang, H.; Li, W.; Yang, H.; Xiong, Y.; Liu, C.; Han, Y.; Yu, Z.-Z.; Li, X. One-Step In Situ Synthesis of a Reduced Graphene Oxide-Based Hybrid Hydrogel for Highly Efficient Water Evaporation and Comprehensive Wastewater Treatment. *ACS Appl. Mater. Interfaces* **2025**, *17*, 46046–46058. [CrossRef]
164. Gao, Z.; Yang, H.; Li, J.; Kang, L.; Wang, L.; Wu, J.; Guo, S. Simultaneous Evaporation and Decontamination of Water on a Novel Membrane under Simulated Solar Light Irradiation. *Appl. Catal. B Environ.* **2020**, *267*, 118695. [CrossRef]
165. Ma, J.; An, L.; Liu, D.; Yao, J.; Qi, D.; Xu, H.; Song, C.; Cui, F.; Chen, X.; Ma, J.; et al. A Light-Permeable Solar Evaporator with Three-Dimensional Photocatalytic Sites to Boost Volatile-Organic-Compound Rejection for Water Purification. *Environ. Sci. Technol.* **2022**, *56*, 9797–9805. [CrossRef]
166. Yan, S.; Song, H.; Li, Y.; Yang, J.; Jia, X.; Wang, S.; Yang, X. Integrated Reduced Graphene Oxide/Polypyrrole Hybrid Aerogels for Simultaneous Photocatalytic Decontamination and Water Evaporation. *Appl. Catal. B Environ.* **2022**, *301*, 120820. [CrossRef]
167. Hao, D.; Yang, Y.; Xu, B.; Cai, Z. Bifunctional Fabric with Photothermal Effect and Photocatalysis for Highly Efficient Clean Water Generation. *ACS Sustain. Chem. Eng.* **2018**, *6*, 10789–10797. [CrossRef]

168. Yang, Y.; Liang, Q.; Al-Dhabi, N.A.; Ya, Y.; Li, J.; Tang, W.; Liu, C. Tilted Evaporator with "1 + 1 + 1 > 3" Synergistic Strengthening in Photothermal, Photocatalytic and Antibacterial Performance for Enhanced Treatment of High-Salinity Dye Wastewater. *Desalination* **2025**, *615*, 119270. [CrossRef]
169. Zhang, B.; Gong, X. Hybrid Hydrogel Evaporators Integrated with the BiOI/Bi_2S_3 Heterojunctions for Enhanced Solar Desalination and Photocatalytic Reduction. *Small* **2025**, *21*, e03889. [CrossRef]
170. Zhu, Z.; Wang, T.; Ren, S.; Feng, Y.; Zhang, Y.; Qian, S.; Tang, W.; Yin, X.; Wu, T.; Gao, S. Construction of Evaporator Based on the Principle of Three Primary Colors to Achieve Synchronous Photothermal Conversion Water Evaporation and Photocatalytic Degradation. *Desalination* **2025**, *606*, 118758. [CrossRef]
171. Yin, M.; Xiao, C.; Jin, Y.; He, Y.; Zhang, Y.; Chen, L. Bionic Solar-Driven Interfacial Evaporator for Synergistic Photothermal-Photocatalytic Activities and Salt Collection during Desalination. *Chem. Eng. J.* **2024**, *499*, 156282. [CrossRef]
172. Fu, A.; Qiu, Z.; Liu, Q.; Chen, Y.; Hu, Y.; Liu, X. Solar-Driven Ti_3O_5/PVA/PAM Frustum-Array Hydrogel Evaporator for Synergistic Water Purification and Photocatalytic Dye Degradation. *Surf. Interfaces* **2025**, *74*, 107654. [CrossRef]
173. Li, W.; Wang, G.; Li, T.; Zhang, Z.; Wang, Y.; Xu, Y.; Sui, W.; Xu, T.; Si, C. All-in-One Self-Cleaning Lignin-Derived Spherical Solar Evaporator for Continuous Desalination and Synergic Water Purification. *Water Res.* **2025**, *282*, 123932. [CrossRef]
174. Li, Z.; Sun, L.; Liu, Y.; Zhu, L.; Yu, D.; Wang, Y.; Sun, Y.; Yu, M. SnSe@SnO_2 Core–Shell Nanocomposite for Synchronous Photothermal–Photocatalytic Production of Clean Water. *Environ. Sci. Nano* **2019**, *6*, 1507–1515. [CrossRef]
175. Mo, H.; Wang, Y. A Bionic Solar-Driven Interfacial Evaporation System with a Photothermal-Photocatalytic Hydrogel for VOC Removal during Solar Distillation. *Water Res.* **2022**, *226*, 119276. [CrossRef]
176. Wang, Z.-Y.; Xu, L.; Liu, C.-H.; Han, S.-J.; Fu, M.-L.; Yuan, B. MXene/CdS Photothermal–Photocatalytic Hydrogels for Efficient Solar Water Evaporation and Synergistic Degradation of VOC. *J. Mater. Chem. A* **2024**, *12*, 10991–11003. [CrossRef]
177. Mulani, S.R.; Bimli, S.; Patil, A.; Jadhav, H.; Miglani, A.; Ma, Y.-R.; Shaikh, P.A.; Devan, R.S. Tri-Functional MFO Nanoparticles for Photocatalytic Complex Dye Removal, Salt-Resistive ISSG Membrane, and Hydrovoltaic Electricity Generation. *Desalination* **2025**, *613*, 119030. [CrossRef]
178. Jia, Z.; Dong, R.; Yang, Y.; Chen, F.; Tang, Y. Rationally Constructing Yolk-Shell Photothermal Material for High-Performance Water Evaporation Coupled with Volatile Organic Compound Degradation. *Chem. Eng. J.* **2025**, *524*, 169502. [CrossRef]
179. Li, J.; Liang, Q.; Yang, Y.; Ya, Y.; Deng, D.; Liu, C. Slide-Shaped Cotton-Based Photocatalytic Solar Evaporator with Dual Mutually Strengthening Functions for Simultaneous Desalination and Dynamic Fast Dye Removal. *Desalination* **2024**, *592*, 118055. [CrossRef]
180. Peng, Y.; Ma, Z.; Ge, B.; Zhao, L.; Zhang, T.; Ren, G.; Zhang, Z. Interfacial Modification Strategies Enhance the Non-Wettability of Bismuth Molybdate and Its Application in Solar Evaporation and Environmental Governance. *Sep. Purif. Technol.* **2025**, *360*, 131202. [CrossRef]
181. Hamza, H.; Diamanti, M.V.; Lughi, V.; Rossi, S.; Meroni, D. Design Efficiency: A Critical Perspective on Testing Methods for Solar-Driven Photothermal Evaporation and Photocatalysis. *Nanomaterials* **2025**, *15*, 1121. [CrossRef]
182. Zhang, L.; Wang, X.; Xu, X.; Yang, J.; Xiao, J.; Bai, B.; Wang, Q. A Janus Solar Evaporator with Photocatalysis and Salt Resistance for Water Purification. *Sep. Purif. Technol.* **2022**, *298*, 121643. [CrossRef]
183. Taranova, A.; Moretti, E.; Akbar, K.; Dastgeer, G.; Vomiero, A. Emerging Strategies to Achieve Interfacial Solar Water Evaporation Rate Greater than 3 $Kg{\cdot}m^{-2}{\cdot}h^{-1}$ under One Sun Irradiation. *Nano Energy* **2024**, *128*, 109872. [CrossRef]
184. Liu, S.; Yang, Q.; Li, S.; Lin, M. A Comprehensive Review of Salt Rejection and Mitigation Strategies in Solar Interfacial Evaporation Systems. *Desalination* **2025**, *600*, 118507. [CrossRef]
185. Sheng, M.; Yang, Y.; Bin, X.; Zhao, S.; Pan, C.; Nawaz, F.; Que, W. Recent Advanced Self-Propelling Salt-Blocking Technologies for Passive Solar-Driven Interfacial Evaporation Desalination Systems. *Nano Energy* **2021**, *89*, 106468. [CrossRef]
186. Zang, L.; Finnerty, C.; Zheng, S.; Conway, K.; Sun, L.; Ma, J.; Mi, B. Interfacial Solar Vapor Generation for Desalination and Brine Treatment: Evaluating Current Strategies of Solving Scaling. *Water Res.* **2021**, *198*, 117135. [CrossRef] [PubMed]
187. Tian, Y.; Wu, P.; Yang, X.; Shi, Y.; Owens, G.; Pi, K. Tailored Iron–Polyphenol Interfacial Networks in Bio-Based Aerogels for Solar-Driven Desalination with Life Cycle Assessment Insights. *Sep. Purif. Technol.* **2025**, *379*, 135118. [CrossRef]
188. Yu, J.; Wang, C.; Liu, S.; Yang, S.; Du, X.; Liu, S.; Shao, C.; Kong, H.; Wang, B.; Wu, T.; et al. Solid Waste-Derived Solar Desalination Devices: Enhanced Efficiency in Water Vapor Generation and Diffusion. *Chem. Eng. J.* **2024**, *485*, 149870. [CrossRef]
189. Yang, Z.; Chen, L.; Chen, Y.; Ju, Y.; Zhang, Z.; Zhang, Z.; Wang, Z.; Chen, C.; Lu, X.; Chen, C.; et al. All-in-One Solar-Driven Evaporator for High-Performance Water Desalination and Synchronous Volatile Organic Compound Degradation. *Desalination* **2023**, *555*, 116536. [CrossRef]
190. Zhu, Y.; Zhang, J.; Jia, S.; Wu, L.; Wang, S.; Wang, W.; Zhang, Y.; Xu, F.; Liu, W. Investigation on Rapid Solar Evaporation, over 100% Evaporation Efficiency, and LCA of a Lotus-like Multi-Layer PVA-Based Aerogel. *Sep. Purif. Technol.* **2025**, *378*, 134505. [CrossRef]
191. Hua, F.; Liu, W.; Li, F.; Hao, W.; Wang, L. Life Cycle Assessment and Energy-Exergy-Economic Performance of Solar Photovoltaic/Thermal Desalination System Integrated with Copper Coils Condensation. *Renew. Energy* **2026**, *256*, 124624. [CrossRef]

192. Siefan, A.; Rachid, E.; Elashwah, N.; AlMarzooqi, F.; Banat, F.; Van Der Merwe, R. Desalination via Solar Membrane Distillation and Conventional Membrane Distillation: Life Cycle Assessment Case Study in Jordan. *Desalination* **2022**, *522*, 115383. [CrossRef]
193. Bahramei, R.; Samimi-Akhijahani, H.; Salami, P.; Behroozi-Khazei, N. Life Cycle Assessment and CFD Evaluation of an Innovative Solar Desalination System with PCM and Geothermal System. *J. Energy Storage* **2025**, *120*, 116116. [CrossRef]
194. Skuse, C.; Tarpani, R.R.Z.; Gorgojo, P.; Gallego-Schmid, A.; Azapagic, A. Comparative Life Cycle Assessment of Seawater Desalination Technologies Enhanced by Graphene Membranes. *Desalination* **2023**, *551*, 116418. [CrossRef]
195. Jijakli, K.; Arafat, H.; Kennedy, S.; Mande, P.; Theeyattuparampil, V.V. How Green Solar Desalination Really Is? Environmental Assessment Using Life-Cycle Analysis (LCA) Approach. *Desalination* **2012**, *287*, 123–131. [CrossRef]
196. Maqsood, M.F.; Fong, K.C.; Ghafoor, F.; Azhar, U.; Rabani, I. Solar Vapor Generation: Advances in Materials Engineering and Structural Design for Efficient Water Evaporation. *Mater. Today Phys.* **2025**, *59*, 101938. [CrossRef]
197. Shi, Y.; Zhang, C.; Li, R.; Zhuo, S.; Jin, Y.; Shi, L.; Hong, S.; Chang, J.; Ong, C.; Wang, P. Solar Evaporator with Controlled Salt Precipitation for Zero Liquid Discharge Desalination. *Environ. Sci. Technol.* **2018**, *52*, 11822–11830. [CrossRef]
198. Wu, F.-J.; Liu, Y.-D.; Wu, S.-M.; Tian, G.; Yang, X.-Y. Towards Durable Photocatalytic Seawater Splitting: Design Strategies and Challenges. *Chem. Commun.* **2025**, *61*, 15087–15103. [CrossRef] [PubMed]
199. Entezami, N.; Farhadian, M.; Davari, N. Removal of Metronidazole Antibiotic Pharmaceutical from Aqueous Solution Using TiO_2/Fe_2O_3/GO Photocatalyst: Experimental Study on the Effects of Mineral Salts. *Adv. Environ. Technol.* **2019**, *5*, 55–65. [CrossRef]
200. Chen, J.; Yin, J.L.; Li, B.; Ye, Z.; Liu, D.; Ding, D.; Qian, F.; Myung, N.V.; Zhang, Q.; Yin, Y. Janus Evaporators with Self-Recovering Hydrophobicity for Salt-Rejecting Interfacial Solar Desalination. *ACS Nano* **2020**, *14*, 17419–17427. [CrossRef]
201. Meng, L.; Shi, W.; Li, Y.; Li, X.; Tong, X.; Wang, Z. Janus Membranes at the Water-Energy Nexus: A Critical Review. *Adv. Colloid Interface Sci.* **2023**, *318*, 102937. [CrossRef]
202. Weng, D.; Xu, F.; Li, X.; Li, Y.; Sun, J. Bioinspired Photothermal Conversion Coatings with Self-Healing Superhydrophobicity for Efficient Solar Steam Generation. *J. Mater. Chem. A* **2018**, *6*, 24441–24451. [CrossRef]
203. Zhang, L.; Li, X.; Zhong, Y.; Leroy, A.; Xu, Z.; Zhao, L.; Wang, E.N. Highly Efficient and Salt Rejecting Solar Evaporation via a Wick-Free Confined Water Layer. *Nat. Commun.* **2022**, *13*, 849. [CrossRef]
204. Xu, X.; Wu, J.; Zhang, J.; Chen, J.; Zhou, Z.; Li, Y.; Yan, Z.; Zhang, J. A 3D Conical Solar Evaporator with Vertically Aligned Microchannels and Diatomite Synergy for High-Efficiency Salt-Resistant Desalination. *J. Mater. Sci.* **2025**, *60*, 15208–15225. [CrossRef]
205. Xiong, L.; Zhan, F.; Liang, H.; Chen, L.; Lan, D. Chemical Grafting of Nano-TiO_2 onto Carbon Fiber via Thiol–Ene Click Chemistry and Its Effect on the Interfacial and Mechanical Properties of Carbon Fiber/Epoxy Composites. *J. Mater. Sci.* **2018**, *53*, 2594–2603. [CrossRef]
206. Yang, M.-Q.; Tan, C.F.; Lu, W.; Zeng, K.; Ho, G.W. Spectrum Tailored Defective 2D Semiconductor Nanosheets Aerogel for Full-Spectrum-Driven Photothermal Water Evaporation and Photochemical Degradation. *Adv. Funct. Mater.* **2020**, *30*, 2004460. [CrossRef]